Aus der Medizinischen Universitätsklinik und Poliklinik Tübingen

Abteilung Innere Medizin II

(Schwerpunkt: Hämatologie, Onkologie, Klinische Immunologie,

Rheumatologie)

Effects of ibrutinib on effector B cells in patients with systemic sclerosis

Inaugural-Dissertation

zur Erlangung des Doktorgrades

der Medizin

der Medizinischen Fakultät

der Eberhard Karls Universität

zu Tübingen

vorgelegt von

Einhaus, Jakob Franz

2021

Dekan: Professor Dr. B. Pichler

1. Berichterstatter: Privatdozent Dr. D. Schneidawind

2. Berichterstatter: Privatdozent Dr. C. Gille

3. Berichterstatter: Professor Dr. J. Distler

Tag der Disputation: 12.03.2021

Table of contents

1   Abbreviations

ACA	anti-centromere antibody
ACR	American College of Rheumatology
ANA	antinuclear antibody
ATA	anti-topoisomerase I antibody (= anti-Scl-70 antibody)
AR	adverse reaction
AS	ankylosing spondylitis
AUC	area under the curve
BAFF	B cell activating factor
Bcl-2	B cell-lymphoma 2
BCR	B cell receptor
Bregs	regulatory B cells
BSA	bovine serum albumin
BTK	Bruton's tyrosine kinase
CD	cluster of differentiation
CI	confidence interval
CLL	chronic lymphocytic leukemia
CpG	cytosine-phosphate-guanin
CT	computed tomography
DAG	diacylglyceride
dcSSc	diffuse cutaneous systemic sclerosis
DMSO	dimethylsulfoxide
DNA	(ds, double strand) desoxyribonucleic acid
ECG	electrocardiography
EDTA	ethylendiamintetraacetate
ELISA	enzyme-linked immunosorbent assay
ERK	(p, phosphorylated) extracellular-signal-regulated kinase
EULAR	European League against Rheumatism
FACS	fluorescence-activated cell sorting
FBS	fetal bovine serum

FDA	food and drug administration
FMO	fluorescence minus one
FSC	forward scatter
GI	gastrointestinal
GvHD	(c, chronic) graft-versus-host-disease
Grb-2	growth factor receptor-bound protein 2
HLA	human leukocyte antigen
HS	human serum
HV	healthy volunteer
IC_{50}	half-maximal inhibitory concentration
ICS	intracellular cytokine staining
IFN-γ	interferon-gamma
Ig	(s, surface) immunoglobuline
IκB	inhibitor of kappa B
IKK	IκB kinase
IL	interleukin
ILD	interstitial lung disease
IP_3	inositol triphosphate
IRAK	interleukin-1 receptor associated kinase
IRF3	interferon regulatory factor 3
ITAM	immunoreceptor tyrosine-based activation motif
lcSSc	limited cutaneous systemic sclerosis
L/D	live/dead
LPS	lipopolysaccharide
MACS	magnetic-activated cell sorting
MAPK	mitogen-activated protein kinase
MCL	mantle cell lymphoma
ME	mercaptoethanol
MFI	mean fluorescence intensity
mRSS	modified Rodnan Skin Score
MyD88	myeloid differentiation primary response 88
NFAT	nuclear factor of activated T-cells

NFκB	nuclear factor of 'kappa-light-chain-enhancer' of activated B cells
PAH	pulmonary arterial hypertension
PBMCs	peripheral blood mononuclear cells
PBS	phosphate buffered saline
PDGF	platelet-derived growth factor
PE	(SA, streptavidin) phycoerythrin
PI	propidium iodide
PKC	protein kinase C
PLC-γ	(p, phosphorylated) phospholipase C gamma
PMA	phorbol 12-myristate 13-acetate
pNF-κB	phosphorylated NF-κB
RA	rheumatoid arthritis
P/S	penicillin/streptomycin
RNA	(m, messenger) ribonucleic acid
rpm	rounds per minute
SCOpE	SCleroderma mOrtality p Eustar
SD	standard deviation
SLE	systemic lupus erythematosus
SMR	standardized mortality ratio
SNP	single nucleotide polymorphism
SRC	scleroderma renal crisis
SSc	systemic sclerosis
SSC	sideward scatter
TAK	transforming growth factor beta-activated kinase 1
TGF	tissue growth factor
TLR	toll-like receptor
TNF	tumor necrosis factor
TRAF	TNF receptor associated factor

2 Introduction

2.1 Systemic sclerosis

Systemic sclerosis (SSc), also known as scleroderma, is a rare autoimmune disease affecting the connective tissue. The fibrosis of the skin and the internal organs by hyperactivation of fibroblasts, vascular damage with luminal narrowing in blood vessels throughout the body and the production of autoreactive antibodies represent the cardinal characteristics of this disease.[1] Clinical symptoms and prognosis can vary greatly between individual cases, mirroring the complex interplay of a multitude of pathological features within an overall poorly understood pathogenesis.

Due to its low prevalence rate between 0.7/100,000 and 53/100,000, depending on the demographics and country, SSc is regarded as an orphan disease.[2] Women are affected more often than men (ratio 4:1), and the mean age of diagnosis is 40 to 50 years. Overall, the prognosis of SSc is highly dependent on the extent of pulmonary, cardiac and renal manifestations. More than 60% of SSc-related deaths were caused by either pulmonary fibrosis or pulmonary arterial hypertension.[3] In a recent meta-analysis from 2014, the standardized mortality ratio (SMR) of SSc was estimated at 2.72 (95% CI: 1.93-3.83) based on 17 studies from 1948 to 2010, and the cumulative survival after diagnosis was calculated to be 74.9% after 5 years and 62,5% after 10 years.[4] Stratifying patients into risk-associated groups in the recently developed SCleroderma mOrtality p Eustar (SCOpE) score allows precise prediction of the 3-year mortality, estimating the survival of high-risk patients (SCOpE ≥ 15) at 53%.[5]

In most cases, Raynaud's phenomenon and skin thickening are amongst the first symptoms to display. Patients experiencing Raynaud's phenomenon describe discolorations of the fingers or toes, usually triggered by cold temperature or stress. Vasal spasms reduce the blood flow, resulting in a white, pale skin color accompanied by numbness or pain. Typically, skin-thickening and edematous

swelling begins in the areas distal to the elbows and manifests symmetrically on both hands. Later, ulcers and scars might develop at the fingertips. Further pathological changes include a mask-like facial expression with microstomia and a shortened lingual frenulum, as well as telangiectasias. At any stage of the disease, involvement of the internal organs, particularly the lungs, heart, kidneys and gastrointestinal (GI) tract (Table 1), can severely aggravate the patient's condition.

Organ	Symptoms
Heart	Myocardial fibrosis Myocarditis Pericarditis
Lung	Interstitial lung disease (ILD) Pulmonary arterial hypertension (PAH) Alveolitis
Kidneys	Arterial hypertonia Chronic kidney disease Kidney infarction
GI tract	Esophageal hypomotility with dysphagia and reflux disease Duodenal hypomotility with meteorism and constipation

Table 1: Organ-specific symptoms of internal organ involvement in SSc.

Corresponding to the extent of skin involvement, two main subtypes of SSc are distinguished: limited cutaneous SSc (lcSSc) and diffuse cutaneous SSc (dcSSc). Typically, lcSSc predominantly affects the skin of the fingers, hands and face and only rarely presents with involvement of the internal organs. In dcSSc, skin fibrosis spreads across the skin of the whole body, often progressing much more rapidly than in lcSSc. Involvement of the internal organs with cardiac, pulmonary, renal and GI complications (Table 2) is much more frequent in dcSSc and usually occurs at an earlier stage.

Items	Subitems	Score
Skin thickening of the fingers of both hands extending proximal to the metacarpophalangeal joints *(sufficient criterion)*	-	9
Skin thickening of the fingers (*only count the highest score*)	Puffy fingers	2
	Sclerodactyly of the fingers (distal to MCP but proximal to the PIPs)	4
Fingertip lesions *(only count the highest score)*	Digital tip ulcers	2
	Fingertip pitting scars	3
Telangiectasia	-	2
Abnormal nailfold capillaries	-	2
PAH and/or ILD	-	2
Raynaud's phenomenon	-	3
Scleroderma related antibodies	Any of anti-centromere, anti-topoisomerase-1 or anti-RNA polymerase III	3
	Max. Total	**24**

Table 2: ACR/EULAR Criteria for the classification of Systemic Sclerosis 2013.[6]

(PAH = Pulmonary arterial hypertension, ILD = Interstitial lung disease). Patients with a score of ≥9 are considered to have definite SSc.

The diagnosis of SSc is based on the 2013 ACR-EULAR classification criteria (Table 2), evaluating clinical symptoms like skin thickening, fingertip lesions, telangiectasia, pulmonary arterial hypertension, abnormal nailfold capillaries and Raynaud's phenomenon, as well as autoantibody status. Patients with a score of ≥9 are considered to have definite SSc. With a sensitivity of 0.91, a specificity of 0.92 and AUC of 0.81 (95-CI: 0.77-0.85) in the validation cohort, this score provides a robust instrument to diagnose SSc.[6] Observed abnormalities in nailfold capillaroscopy achieve a positive predictive value of 81%[7] and can have a significant impact on the diagnostic process. Another important criterion is the testing of patient serum for anti-nuclear antibodies (ANA). More than 94% of patients diagnosed with SSc are positive for ANA.[8] The most frequently detected

SSc-specific ANA include anti-centromere (ACA), anti-topoisomerase (anti-Scl-70, ATA) and anti-RNA polymerase III.[9] Different ANA profiles are associated with certain clinical complications: the presence of anti-Scl-70 autoantibodies correlates with the occurrence of the more severe diffuse form of SSc[10], while anti-RNA polymerase III antibody positive patients have up to 25% greater risk of scleroderma renal crisis.[11] An objective quantification of skin fibrosis is facilitated by using the modified Rodnan Skin Score (mRSS) following the guidelines of the Scleroderma Clinical Trails Consortium.[12] Pulmonary, cardiac, GI and renal manifestations have to be evaluated in separate, organ-specific diagnostic tests (e.g. a pulmonary function test, CT scan, ECG and echocardiography).

On the other hand, genetic indicators play a smaller role and do not have a relevant predictive or diagnostic value, in contrast to other autoimmune diseases such as ankylosing spondylitis (AS). Nevertheless, genetic associations of SSc have been excessively studied and reviewed over the last couple of years.[13] Predominantly human leukocyte antigen (HLA) loci remain a focus of interest in the search for genetic components to SSc susceptibility despite the low concordance rate in monozygotic twins of only 4.7%.[14] Gorlova et al. describe that certain single nucleotide polymorphisms (SNPs) in the HLA-region, namely HLA-DQB1, HLA-DPA1/B1 and NOTCH4, highly correlate with the presence of different types of SSc-specific autoantibodies (ACA, ATA and ACA plus ATA, respectively).[15]

Treatment options for patients with SSc are limited and consist mainly of reactive, symptom-reducing therapies rather than proactive, disease-modifying strategies. In 2017, a task force of experts updated the EULAR recommendations from 2009:[16] A panel of experts evaluated present treatment options, systematically categorized by the efficacy for a specific symptom (e.g. Raynaud's phenomenon, PAH or SRC). For general immunomodulation, patients can temporarily take a systemic glucocorticoid regimen, but careful supervision of kidney function is indispensable due to the increased risk of scleroderma renal crisis under such treatment.[17] Methotrexate, azathioprine, cyclophosphamide and mycophenolate-

mofetil represent alternative strategies for immunosuppression but reliable proof of efficacy has yet to be provided. In case of rapid, life-threatening progression in which the disease cannot be controlled by any drug regimen alongside optimal conservative therapy, pulsed cyclophosphamide and hematopoietic stem cell transplantation have proven to be successful treatment options for patients. A number of randomized controlled trials have shown the efficacy of autologous hematopoietic stem cell transplantation and in a relevant proportion of patients with severe SSc, it can achieve lasting improvement in the patients' condition.[18]

2.2   B cells in the pathogenesis of SSc

Despite many years of intensive research, the pathogenesis of SSc remains incompletely understood. Efforts have been undertaken to unravel the complex interplay between characterized abnormalities that could contribute to the development of SSc. B cells have entered the spotlight over the last decade, as a more prominent role of B cells in the SSc pathogenesis has been suggested. B cells could be pivotally involved in the vascular, fibrotic and immune processes and represent a link between autoimmunity and fibrosis.[19]

B cells or B lymphocytes are a small, but important cell type in the human immune system. Recognition of foreign antigens by B cells and the secretion of the respective antibodies is a crucial instrument of the adaptive immune system's humoral pathogen defense. Furthermore, B cells function as professional antigen-presenting cells and secrete various cytokines. For antigen recognition, B cells express a variable B cell receptor (BCR) on their cell surface. This BCR is composed of a ligand-binding external portion, the surface immunoglobulin (sIg) with a tetramer structure of two heavy (H) and two light (L) chains, and an associated signal transducing portion.[20] B cells derive from pluripotent hematopoietic stem cells in the bone marrow and develop via various lymphoid progenitor cells (Figure 1). In the early stages of B cell development, endless genetic variations of the antigen-binding domain of the sIg are created by ordered rearrangement of the Ig heavy and light chain gen loci via recombination of D-,

J- and V-DNA-fragments.[21] By this diversification of sIg, the immune system builds a repertoire of functional BCR with different VDJ_H and VJ_L, and B cells can recognize an enormous spectrum of antigens.[22] After genetic recombination, every single B cell expresses a genetically unique clone of BCR on its cell surface.
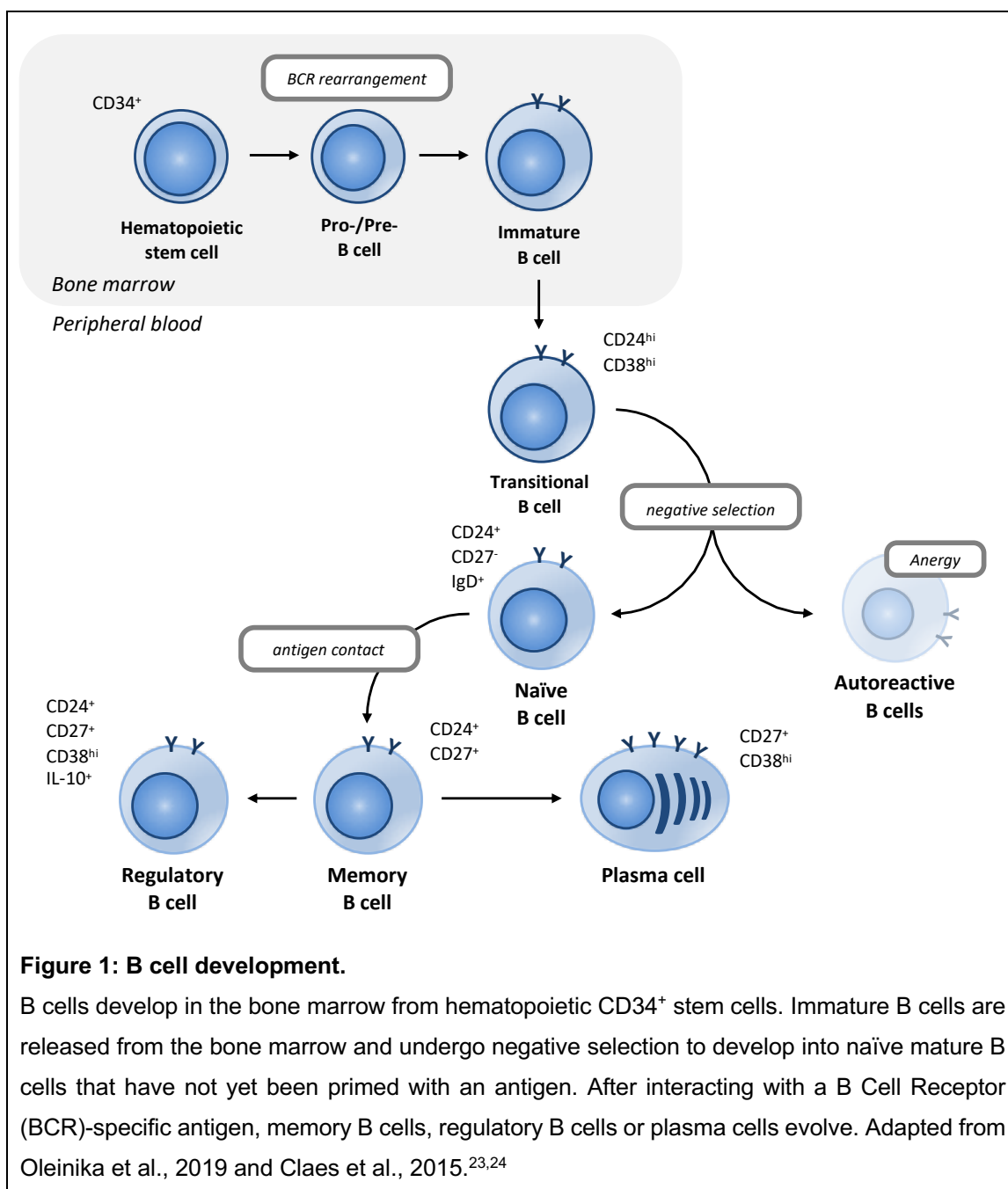
Figure 1: B cell development.

B cells develop in the bone marrow from hematopoietic CD34^{+} stem cells. Immature B cells are released from the bone marrow and undergo negative selection to develop into naïve mature B cells that have not yet been primed with an antigen. After interacting with a B Cell Receptor (BCR)-specific antigen, memory B cells, regulatory B cells or plasma cells evolve. Adapted from Oleinika et al., 2019 and Claes et al., 2015.[23,24]

The immature B cells then undergo the process of negative selection necessary to prevent autoimmune B cells, similar to the negative selection of T cells in the thymus. B cells undergoing this process are at an intermediate stage between immature and mature naïve B cells and are therefore called transitional B cells (CD24^{hi}CD38^{hi}). Matured naïve B cells that have not been exposed to a specific antigen are classified as IgD$^+$CD27$^-$. After antigen exposure, either memory B cells (IgD$^-$ CD27$^+$) or plasmablasts (CD38$^+$CD27^{hi}) evolve.[25] Sato et al. describe that the frequency and the absolute number of B cells are increased in patients with SSc compared to healthy controls by 30%, but they diminish with glucocorticoid treatment.[26] Further analysis of B cell subpopulations revealed that naïve CD27$^-$ B cells were strongly increased in SSc, while memory B cells and plasmablasts were reduced by 35-50% and showed a higher rate of spontaneous apoptosis relative to healthy controls. Despite the numerical reduction of memory B cells and plasmablasts, patients with SSc exhibit autoantibody production in many cases.

Across naïve and memory B cells, the co-stimulatory surface protein CD19 is known to be overexpressed by 20% in patients with SSc.[27] The consequences of altered CD19-expression levels have been investigated in the tight-skin mouse model, a genetic model imitating skin fibrosis and antibody production in SSc. An overexpression of CD19 by two- to threefold has been linked to shifting B cell homeostasis towards the production of autoantibodies; experiments testing a 20% increase in CD19 expression based on the actual level of upregulation in patients have proven to convey a similar effect.[28,29] In contrast, CD19-deficient mice showed no hypergammaglobulinemia as well as less production of profibrotic IL-6 and pathogenetic autoantibodies.[30]

Examples of SSc-specific autoantibodies produced by plasmablasts that have an important functional role in the pathogenesis are anti-PDGF antibodies and anti-Scl-70 antibodies. In previous studies, B cells were found to produce stimulatory antibodies for the PDGF receptor on the surface of fibroblasts and myofibroblasts.[31] Via Ha-Ras, ERK1/2 and ROS, target cells increase collagen-gene expression. Importantly, PDGF antibodies were highly specific for SSc and

were not found in samples of patients with SLE, RA or ILD. Similarly, anti-Scl-70 was shown to bind to the surface of fibroblasts in in vitro assays with subsequent adhesion and activation of SSc monocytic cells.[32] These two B cell-derived mechanisms could be contributing to the induction and maintenance of fibrotic remodeling in skin and internal organs.

The contribution of B cells to skin fibrosis can be explained by the imbalance of functionally distinct B cell subsets. Two functionally antagonistic subsets have been identified, in both the murine and human systems, as the main sources for IL-6 and IL-10, important fibrosis-regulating cytokines. Effector B cells promote autoimmune disease by the production of proinflammatory cytokines such as IL-6, IFN-γ and TNF-α, while regulatory B cells (Bregs) counteract and contain inflammation by releasing IL-10, TGF-β and other anti-inflammatory cytokines.[33] In a mouse model, Matsushita et al. demonstrated that $B^{IL6-/-}$ mice show attenuated cutaneous fibrosis in a Bleomycin-induced scleroderma model, while $B^{IL10-/-}$ mice develop strong skin thickening.[34] Even though IL-10-producing Bregs constitute less than 1% of all B cells in the peripheral blood, they are potent inhibitors of cytokine production via IL-10-dependent pathways.[35] In absence of an exclusive phenotypical marker, the highest proportions of IL-10-producing Bregs exists within the $CD24^{hi}CD27^+$ and the $CD24^{hi}CD38^{hi}$ subpopulations.[35,36] The abundance of Bregs does not follow a uniform trend across all autoimmune diseases. While in systemic lupus erythematosus $CD24^{hi}CD38^{hi}$ Bregs are functionally impaired but not numerically decreased[37], patients with SSc display significantly reduced numbers of IL-10-producing $CD24^{hi}CD27^+$ Bregs.[34] The reduced abundance of Bregs might be the result of a pathologically impaired induction of this subpopulation. Normally, IL-6, IL-21 and the BCR are important activators for the generation of Bregs in the response to inflammation, as the human body reacts to an inflammatory state by increasing pro- and anti-inflammatory agents at the same time.[36] In SSc, the containment of inflammation via anti-inflammatory mediators is insufficient while pro-inflammatory mediators are disproportionally high. Interestingly, when Matsushita et al. followed up on their patients with SSc after an immunosuppressive treatment with

glucocorticoids and/or cyclophosphamide, the numbers of Bregs were significantly increased and disease activity was reduced. This finding is yet another piece of evidence for an imbalance of pro- and anti-inflammatory forces within the immune system in SSc.

Amongst other immune cells like T cells, macrophages and monocytes, as well as mesenchymal cells like endothelial cells and fibroblasts, B cells have great potential to influence the inflammatory state via the production of cytokines. A study screening the plasma cytokine levels of 444 patients with SSc by Gourh et al. revealed elevated levels of IL-6, TNF-α and IFN-γ compared to healthy controls, all of which can be produced by B cells upon activation.[38] IL-6 is a prototypical proinflammatory cytokine that can induce the expression of collagen in fibroblasts through direct and indirect mechanisms.[39] Inhibition of IL-6 transduction, therefore, was suggested as a therapeutic approach in SSc.[40] The IL-6-receptor antibody tocilizumab can effectively avert IL-6 functions and is clinically employed in the treatment of RA. In a recent phase II, randomized and controlled clinical trial, tocilizumab failed to show significant improvement for the primary endpoint (mRSS), even though a trend towards slowing down disease progress was observed in a couple of secondary endpoints.[41] Similarly, the TNF-α blocking antibody infliximab has been tested in SSc for clinical improvement in a pilot study, but it only showed a trend toward lower mRSS and a reduction of collagen production of fibroblasts in vitro.[42] TNF-α is an important mediator in local inflammation and shares many functions with IL-6 as it influences cell differentiation, activation and apoptosis via the central transcription factor NFκB.

Inversely, IL-6 and TNF-α are also important players in B cell activation. Both cytokines promote the production of immunoglobulins in an autocrine manner, while in the presence of neutralizing antibodies for either IL-6 or TNF-α, stimulated B cells produced less IgG and IgM.[43] The role of IFN-γ in SSc is a subject of a controversial discussion. On one hand, IFN-γ can inhibit collagen synthesis in fibroblasts[44], and elevated levels of IFN-γ might be a reaction to the

reduced sensitivity of fibroblasts to IFN-γ in SSc.[45] However, higher levels of IFN-γ were also shown to correlate with certain autoantibodies in SSc, namely ATA and anti-U1RNP.[46]

Overall, B cells have been identified as key players in the pathogenesis of SSc and, therefore, have been the target of different therapeutic approaches. Rituximab, a CD20-antibody that is used in order to deplete neoplastic B cells in B cell malignancies, has been tested in a phase II clinical trial.[47] As this study failed its primary end point, theories were put forward to explain this lack of effectiveness. Most importantly, the nonselective depletion with an emerging aggravated deficit of Bregs is suspected to be a critical weakness of this therapeutic approach.[48] A more biased intervention acting predominantly against the subset of proinflammatory effector B cells, functionally classified as IL-6$^+$ B cells, while sparing Bregs, could present a great advance in addressing B cell pathology in SSc.

2.3 Bruton's tyrosine kinase inhibitor ibrutinib and BCR signaling

Ibrutinib (formerly PCI-32765, Figure 2) was developed by a team of scientists at Celera Genomics in 2006 as a small molecule inhibitor of Bruton's Tyrosine Kinase (BTK).[49] The irreversible inhibition of BTK as an important component of the BCR signaling pathway seemed of high interest in B cell malignancies and autoimmune diseases with an

Figure 2: Molecular structure of ibrutinib
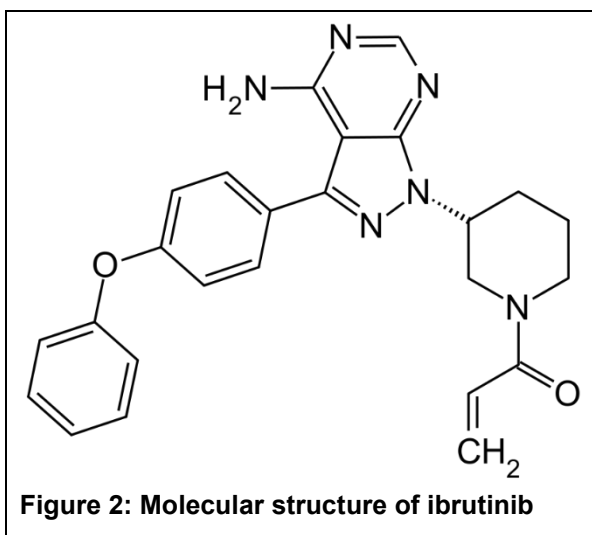
important role for B cells. Even though benefits in autoimmune diseases were assumed from the very beginning, to date official FDA approved clinical applications are mostly limited to relapse situations of B cell malignancies, namely chronic lymphocytic leukemia (CLL), Morbus Waldenstrom and mantle

cell lymphoma (MCL).[50–52] In 2017, ibrutinib was approved as a second-line therapy for chronic graft-versus-host disease (cGvHD), a disease sharing many clinical and pathological features with SSc.

In both cGvHD and SSc, B cells are suspected to fundamentally contribute to disease development and perpetuation. In cGVHD, B cells are dysregulated showing a higher resistance to apoptosis[53], they are functionally and morphologically altered through exposure to increased levels of BAFF[54], and can produce donor-derived alloantibodies. In 43 to 83% of cases, patients with cGvHD responded to treatment with the anti-CD20 antibody, rituximab, depleting the pathologically altered B cells.[55] This provided the rational for the use of ibrutinib, as it inhibits B cell activation and survival. After Dubovsky et al. had shown that ibrutinib positively influenced the clinical manifestations of chronic GvHD in a murine model[56], a clinical trial stage 1b/2 conducted with patients who had failed to show adequate improvement under a glucocorticoid-based, first-line regime proved to be a success.[57]

When a B cell's BCR binds a matching foreign antigen, the B cell is activated and might start to proliferate and differentiate. In the context of an invasive pathogen, B cells are needed as producers of highly specific antibodies to fight off the infection. B cell activation can thereby be T cell-dependent or T cell-independent.[58] While T cell-dependent activation is based on a complex interplay of helper T cells and B cells and is localized mostly in the lymphoid follicles of the spleen and lymph nodes, T cell-independent activation provides a mechanism for B cells to react rapidly to antigens like bacterial components. For the latter, the BCR cooperates with toll-like receptors (TLR) such as TLR7 or TLR9 and facilitates the delivery of ligands to their respective receptors.[59–61]
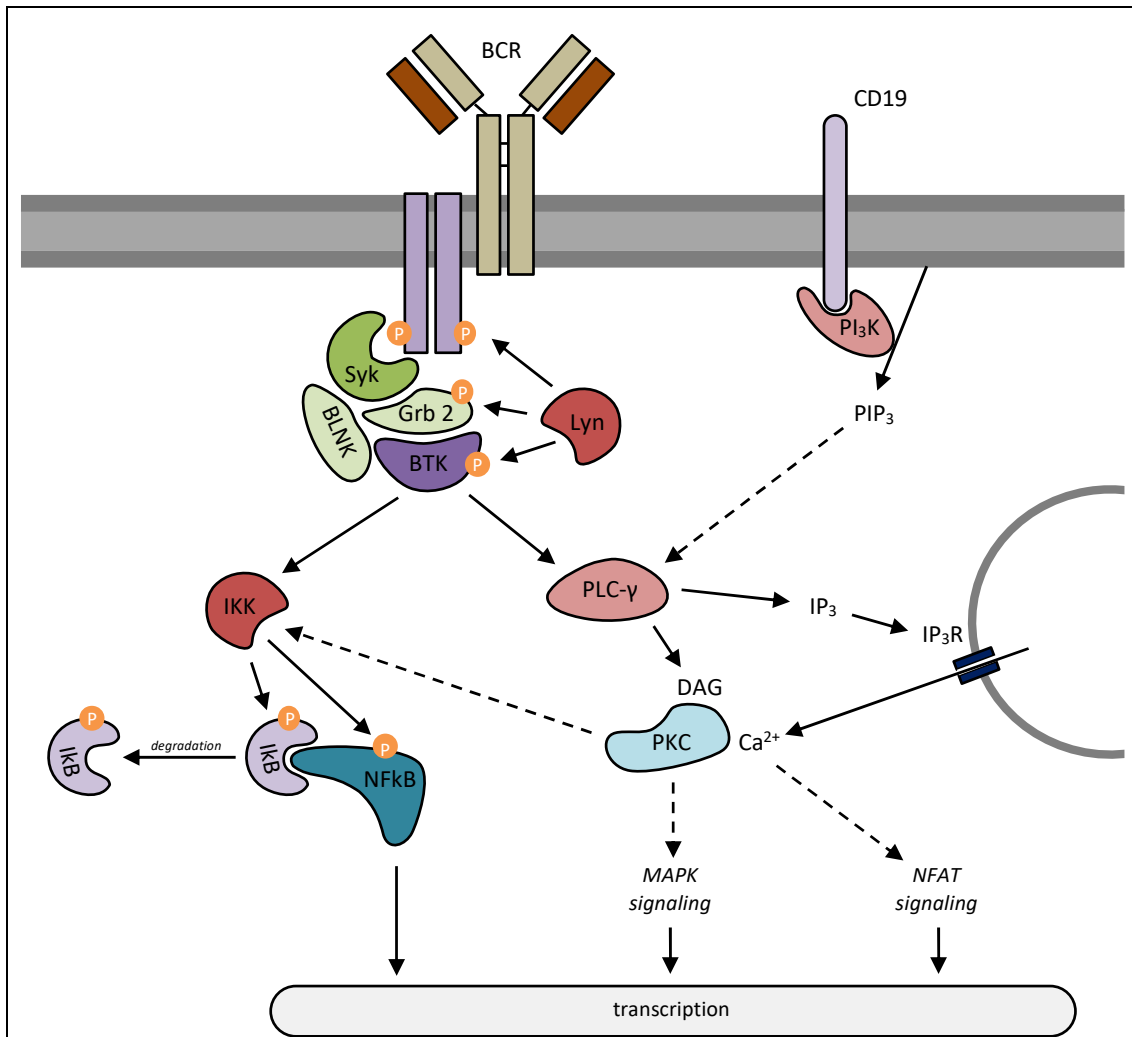
Figure 3: Involvement of Bruton's Tyrosine Kinase (BTK) in BCR signaling.

BTK mediates the effects on transcription downstream of the BCR mainly through the kinases IKK and PKC and the phosphorylated transcription factors NFκB, NFAT and MAPK. CD19, a surface molecule on B cells, is involved in the BCR signaling pathway as an amplifier of signal transmission. Adapted from Merolle et al., 2018.[62]

The intracellular domain of the BCR, consisting of an Igα-Igβ heterodimer, is phosphorylated upon activation by Lyn, an Scr family kinase, enabling the Syk kinase to bind to the phosphorylated immunoreceptor tyrosine-based activation motif (ITAM) (Figure 3). BTK, Grb 2 and BLNK are recruited by Lyn to form the BCR signalosome and they are activated by Syk.[62] In particular BTK plays a pivotal role in amplifying BCR signaling. A BTK loss-of-function mutation causes the X-linked agammaglobulinemia with deficient antibody production and

impaired memory B cells.[63] BTK activates the IκB kinase that phosphorylates IκB, thereby enabling the nuclear translocation of NFκB.[64] Furthermore, BTK activates the phospholipase C-γ2 (PLC-γ2), facilitating Ca^{2+} influx via inositoltriphosphate (IP_3) and activation of protein kinase C (PKC) through Ca^{2+} and diacylglycerin (DAG).[65] Ultimately, the main transcription factors downstream of the BCR are NFAT (via Ca^{2+} influx), NFκB (also activated by PKC) and, to a lesser extent, ERK.[62]

Within this signaling cascade, ibrutinib binds covalently to Cys-481 in the active site of BTK for potent (IC_{50} = 0.5 nM) and highly selective inhibition, as well as observable downstream effects, such as a lower availability of pPLC-γ2 and pERK.[66]

2.4 TLR9 signaling pathway

The TLR family recognizes molecular patterns associated with pathogens to kickstart an adequate innate immune response. Unlike other TLRs (TLR1, 2, 4, 5 and 6) that are located on the cell surface, the inactive TLR9 is positioned in the membrane of endosomes.[67] TLR9 can facilitate T cell-independent BCR activation but also initiates an intracellular signaling cascade on its own. It is activated by binding of internalized dsDNA, specifically unmethylated cytosine-phosphate-guanin (CpG) motifs within the DNA.[68] Even though these motifs are more abundant in viral and bacterial than in mammalian (self-) DNA, a pathogenetic role of TLR9 signaling has been suggested in SSc.[69,70] Interestingly, hypomethylation of CpG motifs has been reported in the DNA of CD4^{+} T cells and fibroblasts of patients with SSc.[71,72] This finding supports a possible role for self-DNA-triggered activation of autoreactive B cells via TLR9 in the context of autoimmunity, as first shown in vitro by Leadbetter et al.[73]

DNA fragments are internalized into the tubular lysosomal compartment and subsequently bind directly to TLR9.[74] Myeloid differentiation primary response 88 (MyD88) is accumulated in an oligomer structure and recruits IRAK4 and IRAK1

or 2 to form the myddosome complex (Figure 4).[75] After autophosphorylation within this complex, IRAK1 is released and associates with the ubiquitin ligase TRAF6, resulting in NFκB- and MAPK-signaling via activation of TAK1 kinase.[76] This signaling pathway is at least partly dependent on BTK function, which proved necessary for the induction of the NFκB-target gene IL-6 via TLR9.[77,78]
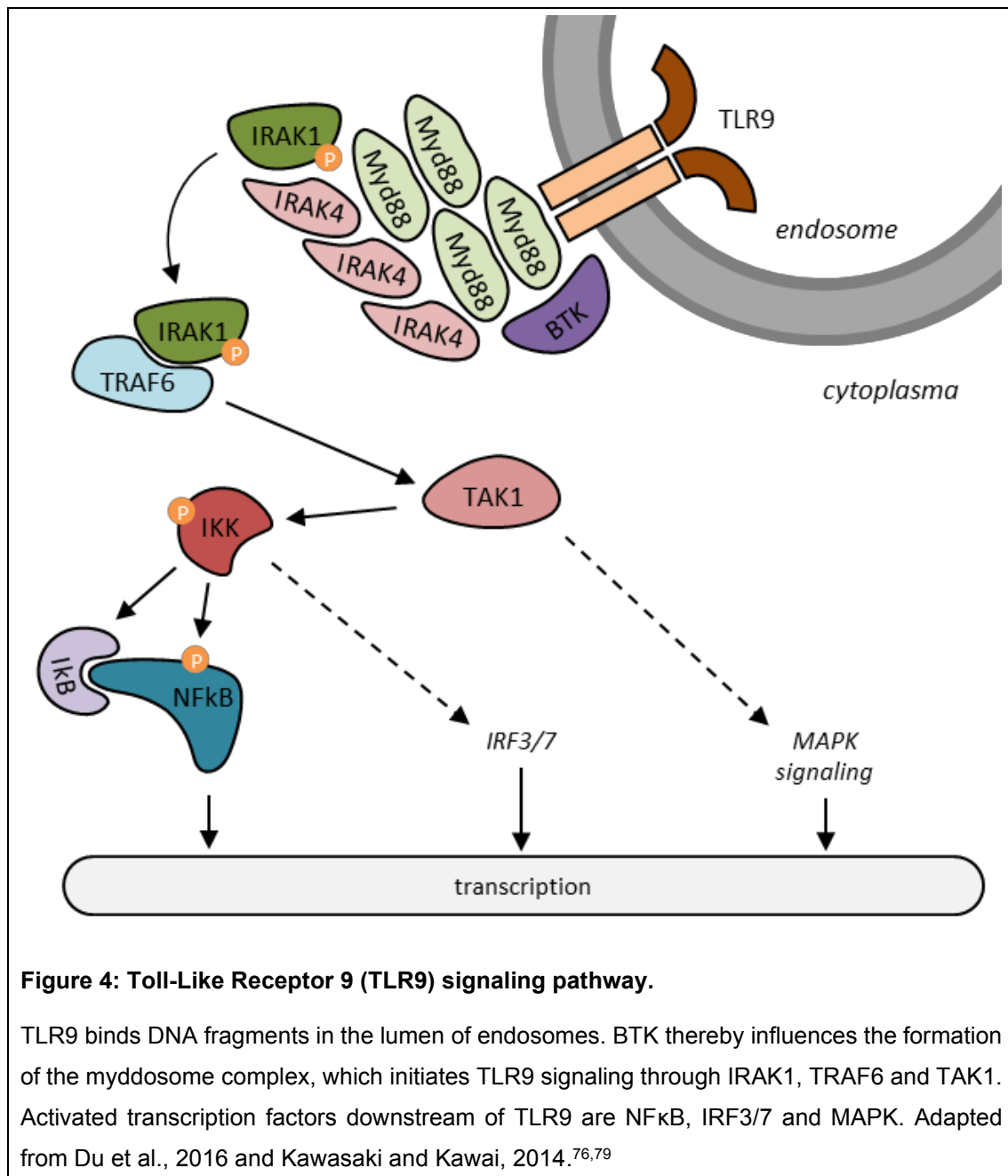
Figure 4: Toll-Like Receptor 9 (TLR9) signaling pathway.

TLR9 binds DNA fragments in the lumen of endosomes. BTK thereby influences the formation of the myddosome complex, which initiates TLR9 signaling through IRAK1, TRAF6 and TAK1. Activated transcription factors downstream of TLR9 are NFκB, IRF3/7 and MAPK. Adapted from Du et al., 2016 and Kawasaki and Kawai, 2014.[76,79]

2.5 Objective

Ibrutinib has been suggested as a potential therapy in autoimmune diseases in which B cells play an important role. In this investigation, ibrutinib was tested on samples of patients with SSc in an in vitro model of TLR9-mediated autoimmunity, evaluating the effects of ibrutinib treatment on cytokine production, transcriptional activity and autoantibody production. The TLR9-agonist CpG was used to imitate sterile inflammation and to induce an immunological response in B cells. These preliminary, in vitro tests will examine the potential of ibrutinib in the context of SSc and help determine whether the clinical application of ibrutinib could prove beneficial for patients with SSc.

3 Materials and methods

3.1 Materials

3.1.1 Chemicals and reagents

Chemical/reagent	Distributor
Dulbeccos Phophate Buffered Saline (PBS)	Gibco, New York, US
Dimethylsulfoxid (DMSO)	Sigma-Aldrich, St. Louis, US
Fetal Bovine Serum (FBS)	Biochrom, Berlin, Germany
RPMI 1640 (1X) + Glutamax	Gibco, New York, US
Penicillin/Streptomycin (P/S)	Lonza, Basel, Switzerland
Hepes Buffer	Gibco, New York, US
Sodium pyruvate 100 mmol	Gibco, New York, US
Tryptan blue (0.4%)	Sigma-Aldrich, St. Louis, US
Bovine Serum Albumin (BSA)	Biomol, Hamburg, Germany
Ethylendiamintetraacetate (EDTA)	Sigma-Aldrich, St. Louis, US
Human Serum (HS)	C-C-Pro, Oberdorla, Germany
MEM NEAA	Gibco, New York, US
2-Mercaptoethanol (ME)	Sigma-Aldrich, St. Louis, US
Methanol (100%)	Merck, Darmstadt, Germany

Table 3: Chemicals and reagents

3.1.2 Stimuli

Stimuli	Distributor
Lipopolysaccharide (LPS)	Sigma-Aldrich, St. Louis, US
Oligonucleotide CpG (ODN2006)	Invivogen, San Diego, US
Cell stimulation cocktail (PMA/Ionomycin + Monensin A/Brefeldin)	Thermo Fisher Scientific, Waltham, US

Table 4: Substances used for cell stimulation

3.1.3 Antibodies

Antigen	Clone	Color	Concentration	Distributor
CD3	HIT3a	PerCP-Cy5.5	1:400	Biolegend, San Diego, US
CD20	2H7	BV510	1:200	Biolegend, San Diego, US
CD27	O323	BV421	1:200	Biolegend, San Diego, US
IgD	IA6-2	FITC	1:200	Biolegend, San Diego, US
CD24	ML5	BV650	1:100	BD Bioscience, Franklin Lakes, US
CD38	HIT2	PE-Dazzle	1:100	Biolegend, San Diego, USA
IL-6	MQ2-13A5	PE-Cy7	1:100	Biolegend, San Diego, USA

Table 5: Antibody panel "Intracellular cytokine staining"

Antigen	Clone	Color	Concentration	Distributor
CD3	OKT3	BV605	1:400	Biolegend, San Diego, USA
CD19	HIB19	BV421	1:200	Biolegend, San Diego, USA
pNFKB (rabbit)	93H1	-	1:1600	Cell Signaling, Boston, USA
Anti-rabbit	**Fab2**	**PE-Cy7**	**1:800**	Cell Signaling, Boston, USA

Table 6: Antibody panel "Phosphoflow"

3.1.4 Media and buffers

Medium/Buffer	Reagent (Concentration)
B cell culture medium	RPMI 1640 (1X) + Glutamax HS (10%) P/S (1%) Hepes Buffer (1%) MEM NEAA (1%) Sodium pyruvate (1%) 2-ME (5.5 µM)
Freezing medium	RPMI 1640 (1X) + Glutamax FBS (20%) DMSO (10%)
MACS Buffer	PBS BSA (0.5%) EDTA (2 mM)
FACS Buffer	PBS FBS (2%)

Table 7: Medias and buffers

3.2 Patient cohort

Patients with SSc were recruited consecutively at the Department of Medicine II at Tuebingen University Hospital from 2016 to 2019. Written consent was obtained from all patients prior to drawing 40-100 ml of peripheral blood in heparinized tubes. A positive vote of the ethics committee of the Medical Faculty Tuebingen was obtained (vote: 114/2016BO2) according to the declaration of Helsinki (1975, revised in 2013). Buffy coats of healthy donors that served as controls were received from the blood bank at the Tuebingen University Hospital.

3.3 Methods

Cell cultures were incubated at 37°C, 95% relative humidity and 5.0% CO_2. To determine the live cell count, cells were dyed with tryptan blue and counted in a Neubauer counting chamber (Brand, Wertheim, Germany) with an Axiovert 25 microscope (Zeiss, Jena, Germany). Default parameters of centrifugation for washing steps were 5 minutes and 1500 rpm.

3.2.1 PBMC extraction from patient samples and buffy coats

The Peripheral Blood Mononuclear Cells (PBMCs) were extracted from patient samples and buffy coats via FICOLL separation. Patient samples (~75 ml whole blood) were diluted in PBS in a ratio of 1:3. Buffy coats (25 ml of concentrated leucocytes) were diluted in PBS to a total volume of 210 ml. The diluted samples were cautiously layered over FICOLL separating solution (Biochrom AG, Berlin, Germany). The different cell types were sorted into layers of equal density by centrifugation (20 minutes at 2000 rpm, with the brake turned off). The interphase containing concentrated PBMCs was collected in new tubes and washed twice with PBS. A third washing step with PBS followed by centrifugation for 10 minutes at 800 rpm, leaving the thrombocytes in the supernatant to discard, was performed. The cell pellet was dissolved in PBS and counted, and then re-diluted in freezing medium to an appropriate concentration of between 5 and 100x10^6

cells/ml. The samples were aliquoted in 1ml cryovials and frozen at -80°C in a propanol tank, then transferred to liquid nitrogen until further use.

3.2.2 Purification of B cells by magnetic cell separation

Magnetic-Activated Cell Sorting (MACS) was used to purify B cells from the cryo-preserved PBMCs of patients or healthy volunteers (buffy coats). PBMCs were thawed for a maximum of 90 seconds in a 37°C water bath and suspended in 50ml PBS. The cells were pelleted and counted, then dissolved in 800µl of MACS buffer and 100µl of CD19 MicroBeads (Milteny-Biotec, Bergisch Gladbach, Germany) per 100×10^6 cells for an incubation of 15 minutes at 4°C.

The stained cell suspensions were washed with 2 ml of MACS buffer per 100×10^6 cells and resuspended in 500 µl of buffer per 100×10^6 cells. MACS LS Columns (Miltenyi Biotec, Bergisch Gladbach, Germany) were placed in the magnetic field of the QuadroMACS Separator (Miltenyi Biotec, Bergisch Gladbach, Germany) and primed with 3 ml of MACS buffer. The cell suspension was pipetted onto the column and washed through in three washing steps of 3 ml of MACS buffer each. To collect the magnetically labeled cells stuck in the column, the column was removed from the magnetic field of the MACS separator, placed on a 15 ml Falcon tube and flushed with 5 ml of MACS buffer.

3.2.3 In vitro ibrutinib assay in PBMCs

PBMCs from healthy donors and patients with SSc were incubated with ibrutinib for 24 hours to evaluate changes in the production of IL-6 via intracellular cytokine staining. Samples were thawed and preincubated at 2×10^6 cells/ml with ibrutinib for 1 hour and then resuspended at 1×10^6 cells/ml on a 48 well plate (1 ml/well). The PBMCs were treated with medium (control), a TLR4-agonist (LPS, 10 µg/ml) or a TLR9-agonist (CpG, 0.1 µg/ml) for a 24-hour period. For the last 4 hours of culture, a cell stimulation cocktail containing phorbol 12-myristate 13-acetate (PMA) and ionomycin in combination with Monensin A and Brefeldin

(eBioscience™ cell stimulation cocktail) was added. The protocol for intracellular cytokine staining was started immediately after the 24-hour culture.

3.2.4 In vitro ibrutinib assay in a culture of purified B cells

The effects of the BTK inhibitor ibrutinib on B cells were tested in vitro on samples from healthy donors and patients with SSc. Purified B cells were preincubated with ibrutinib for 1 hour at a concentration of $2x10^6$ cells/ml before the setup of a B cell culture for 24 or 72 hours, respectively, on a 96 well plate (200 μl/well, $1x10^6$ cells/ml). B cells were either left unstimulated or were treated with LPS (10 μg/ml) or CpG (1 μg/ml). After 24 or 72 hours, respectively, supernatant was harvested and frozen at -20°C until further analysis. Alternatively, a cell stimulation cocktail containing PMA and ionomycin in combination with Monensin A and Brefeldin (eBioscience cell stimulation cocktail) was added for the last 4 hours of culture allowing for the detection of intracellular cytokine production.

3.2.5 Viability assay on B cells of healthy donors

To determine the effects of ibrutinib on B cell viability in this 24-hour in vitro model, B cell cultures of samples from three healthy donors were set up as described in 3.2.4. During the last step of staining, 3 μm polystyrene latex counting beads (Sigma-Aldrich St. Louis, US) were added to the samples. An SSC/FSC gate on the counting beads was used as a stopping gate to record a consistent number of beads throughout all samples. Thus, absolute B cell numbers could be compared between different samples.

3.2.6 Intracellular cytokine staining

In order to detect cytokine production on a single cell level, a protocol for the optimal investigation of IL-6 production in B cells was established. For optimal fluorescence results, the antibody panel "Intracellular cytokine staining" (ICS) was titrated and used at the concentrations listed in Table 5. The 24-hour in vitro model was chosen based on a comparison of the timepoints 6 hours, 24 hours

and 72 hours and oriented following protocols previously described in literature[48]. For a robust detection of IL-6, PMA and ionomycin were added for the last 4 hours of culture in combination with Monensin A and Brefeldin (eBioscience cell stimulation cocktail), two inhibitors of the Golgi apparatus trapping cytokines in vesicles inside the cell. The use of Monensin A and Brefeldin alone was not sufficient to detect reliable levels of IL-6$^+$ cells under TLR-stimulation (Figure 5A and B).

Figure 5: IL-6+ B cells with PMA/Ionomycin stimulation

In order to establish an optimal ICS protocol, B cell cultures were treated with the Golgi inhibitors Monensin A and Brefeldin alone or in combination with PMA and ionomycin. Both in unstimulated (**A**) and LPS-stimulated (**B**) samples, a robust induction of IL-6$^+$ B cells was achieved with PMA/ionomycin treatment. Numbers indicate percentage of all B cells within the depicted gate.

After culture, the cells were harvested and transferred to FACS tubes. The individual samples were washed with FACS buffer, incubated with Fc-receptor block (1:100 in FACS buffer) for 5 minutes at 4°C and then stained with a master mix of antibodies for surface antigens and a fixable viability dye eFluor780 (eBioscience) for 20 minutes. The cells were fixed (eBioscience™ IC Fixation Buffer) at room temperature in the dark for 30 minutes and permeabilized (eBioscience™ IC Perm Buffer). Again, Fc receptors were blocked for 10 minutes at room temperature before staining the samples for the intracellular antigens (30 minutes at room temperature). The excess antibodies were washed off and the cells were stored at 4°C until measuring at the flow cytometer.

3.2.7 Intranuclear NFκB staining

PBMC cultures of healthy donors and patients with SSc were set up as described in 3.2.3. After 20 hours, the eBioscience cell stimulation cocktail was added to the culture for 1 hour. The samples were transferred to FACS tubes and washed with FACS buffer. Fc-Block (1:100 in FACS buffer) was added for 5 minutes prior to staining the cells with a master mix of antibodies for surface antigens (Table 6) and a fixable viability dye eFluor780 (eBioscience) for 20 minutes. After fixation with IC Perm Buffer (eBioscience) for 15 minutes, the cells were permeabilized with 100% ice-cold methanol for 45 minutes. In BSA buffer, Fc receptors were blocked, then pNFκB was stained with a rabbit-anti-pNFκB antibody for 30 minutes at room temperature. An anti-rabbit PE-Cy7 antibody served as secondary antibody (30 minutes, room temperature). Before measuring the samples at the flow cytometer, surplus antibody was washed off with BSA buffer twice.

3.2.8 Flow cytometry

Flow cytometry was used to identify and differentiate immune cell subsets dependent on their expression of surface markers. Focused to a single cell stream, the cells pass a number of lasers in the flow cytometer stimulating the fluorochromes conjugated to the antibodies. The emitted fluorescence signals are detected and can be assigned by wavelength to the originating fluorochrome. All samples were measured using an LSR II Fortessa flow cytometer (BD Biosciences, Franklin Lakes, USA). Compensation for all used antibody panels was performed using One Comp eBeads (eBioscience) and the FlowJo software.

3.2.9 Legendplex assay

For the analysis of cytokines in the culture supernatant, a Mix-and-Match Biolegend Multi-Analyte Flow Assay Kit (LEGENDplex™) was used quantifying IL-6, IL-10, TNF-α, IFN-γ, IL-21 and IL-4. In this bead-based flow-cytometry assay for cytokine detection, the analyte is bound by analyte-specific capture beads and biotinylated detection antibodies forming a sandwich formation as in other

immunoassays, such as ELISA. The detection antibodies are then bound by a streptavidin-PE-antibody. The beads for every individual analyte are distinguished by bead size (two sizes: A and B) and internal fluorescence intensity. The PE-signal is proportional to the amount of captured analyte.

The protocol provided by Biolegend served as a basis for use, with little modifications to the procedure. Incubation was performed at room temperature on a plate shaker (250 rpm). A V-bottom plate was loaded with 15µl of assay buffer, the 15 µl of the standard dilution series (C7 = 10.000 pg/ml, C6 = 2.500 pg/ml, C5 = 1.250 pg/ml, etc., C0 = 0.0 pg/ml) or 15 µL of the analyzed sample were added, respectively. Next, 15 µl of a 1X mix of all capture beads was added, then the plate was sealed with a plate sealer, wrapped in aluminum foil and incubated for 2 hours. The plate was centrifuged at 1100 rpm for 5 minutes collecting the beads at the very bottom of the V-shaped wells, allowing to flick off the superfluous liquid. The beads were washed with 200 µl of wash buffer per well, and 15 µl of detection antibody was added. After 1 hour of incubation, the SA-PE antibody was directly added to the wells without another washing step and the samples were incubated for 30 minutes. The samples were washed again, then the beads were resuspended in 150 µl of wash buffer to be measured using a BD FACSLyric (BD Biosciences, Franklin Lakes, USA).

3.4   Data analysis

For analysis of all flow cytometry data, the FlowJo software (Tree star, version 10.2) was used. Statistical analysis was performed in GraphPad Prism (GraphPad Software, version 7.01). Multiplex data was analyzed using the Legendplex software (Biolegend, version 8.0). All data points represent the calculated means of technical duplicates. To test for intraindividual differences, a paired student t-test was used to calculate significance. For analysis comparing data sets from healthy volunteers and patients with SSc, an unpaired student t-test was used to calculate p-values. ANOVA tests were performed when testing multiple parameters. Statistical significance was assumed for $p < 0.05$ (* = p<0.05, ** = p<0.01, *** = p<0.001, **** = p<0.0001).

4 Results

4.1 Differential effects of ibrutinib in the context of TLR-stimulation of B cells in healthy volunteers

In the process of establishing a reliable model of autoimmune inflammation, changes to the cytokine profile of B cells with ibrutinib treatment were investigated in the context of TLR4- and TLR9-stimulation in healthy volunteers.
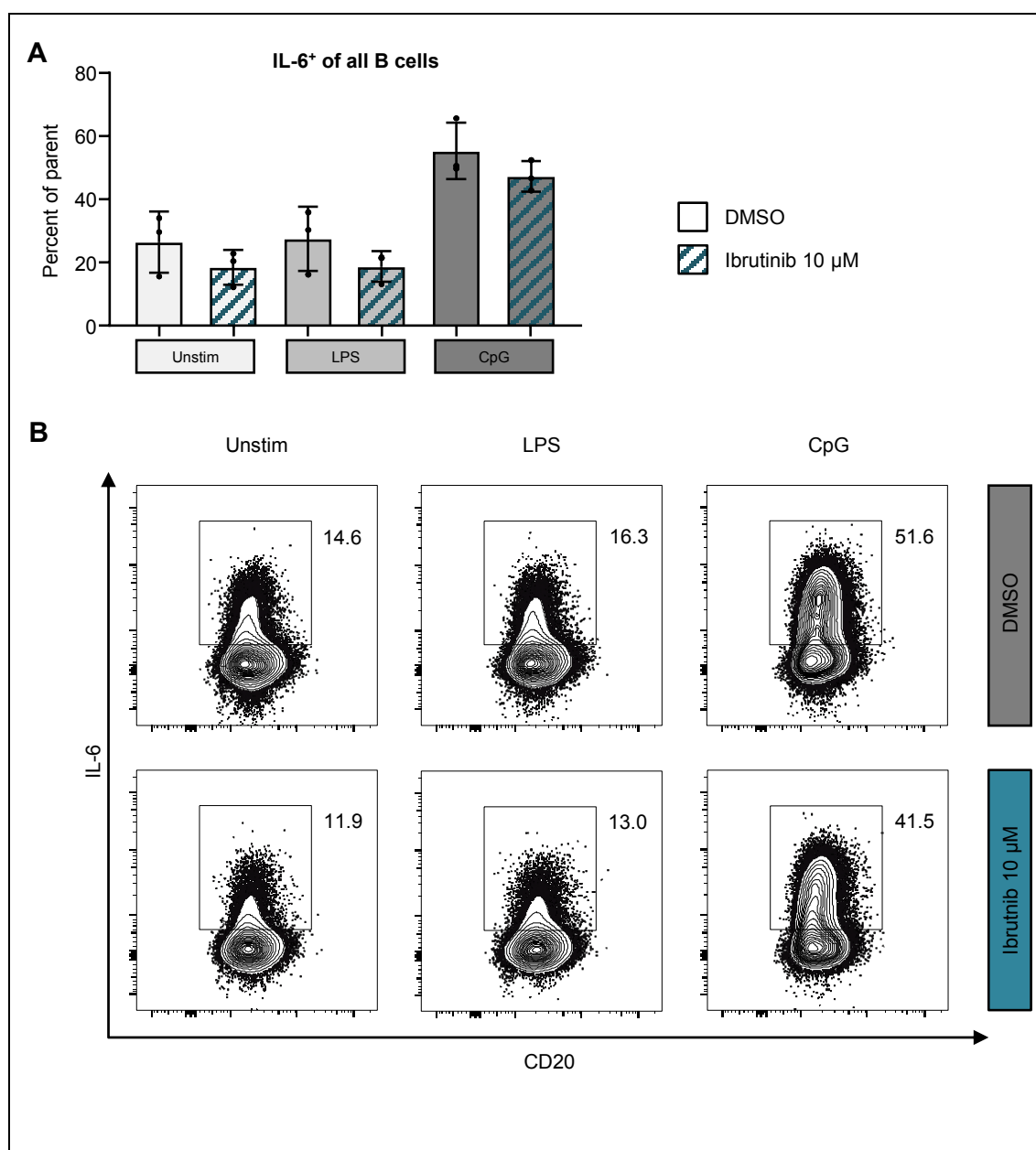
Figure 6: Intracellular IL-6 staining in B cells from healthy volunteers comparing ibrutinib treatment with LPS- and CpG-stimulation

Intracellular IL-6 was stained in B cells from healthy volunteers after 24 hours of culture (*n=3*). The influence of ibrutinib on IL-6-production was tested in unstimulated, LPS-treated and CpG-stimulated samples. **A.** Proportion of IL-6$^+$ B cells of all B cells is depicted. Significance was calculated using a paired student's t-test. Bars represent mean, error bars depict SD. * = p<0.05, ** = p<0.01. **B.** Representative flow cytometry dot plots from one HV show the percentage of IL-6$^+$ B cells of all B cells.

Initially, intracellular cytokine staining was used to determine the production IL-6 in B cells. In unstimulated samples, 26.5 ± 9.7% of all B cells were IL-6$^+$ and 10 µM ibrutinib reduced the ratio to 18.5 ± 5.5% (Figure 6A and B). LPS-treatment only slightly increased the percentage of IL-6$^+$ B cells to 27.5 ± 10.2%, while ibrutinib still achieved a comparable reduction to 18.7 ± 4.8%. In CpG-stimulated samples, 10 µM ibrutinib conveyed a reduction of IL-6$^+$ B cells from 55.3 ± 9.0% (DMSO control) to 47.3 ± 4.8%. As LPS induced only a small increase in IL-6 production in this experiment, it was assumed that a high amount of the detected IL-6 was produced in response to the stimulation with PMA and ionomycin during the ICS protocol.

In order to exclude any influence of this additional cell stimulation, a Legendplex assay was used to analyze the cytokines released into the culture supernatant with and without ibrutinib (10 µM) under LPS- and CpG-treatment and in unstimulated controls (Figure 7A-D). In unstimulated samples, IL-6, TNF-α and IL-10 were barely released; only IFN-γ was detected in considerable doses. In comparison, both LPS and CpG clearly induced an increased production of IL-6, TNF-α and IL-10, with LPS generally effecting the greater increase. Under CpG-stimulation, ibrutinib uniformly reduced the production of cytokines: IL-6 levels were reduced from 559.7 ± 41.5 pg/ml to 341.4 ± 6.1 pg/ml (p = 0.009), TNF-α from 85.1 ± 46.4 pg/ml to 35.9 ± 9.4 pg/ml, IFN-γ from 33.0 ± 26.0 pg/ml to 26.5 ± 16.7 pg/m and IL-10 from 6.3 ± 6.7 pg/ml to 3.9 ± 2.8 pg/m.

Interestingly, ibrutinib actually increased IL-6 levels from 1640 ± 1520 pg/ml to 2118 ± 1596 pg/ml under LPS stimulation (p = 0.047). TNF-α, IFN-γ and IL-10 were reduced from 148.8 ± 130.0 pg/ml to 92.9 ± 52.2 pg/m, from 26.8 ± 21.1 pg/ml to 22.9 ± 25.7 pg/m and from 16.0 ± 20.4 pg/ml to 10.3 ± 12.2 pg/m respectively.
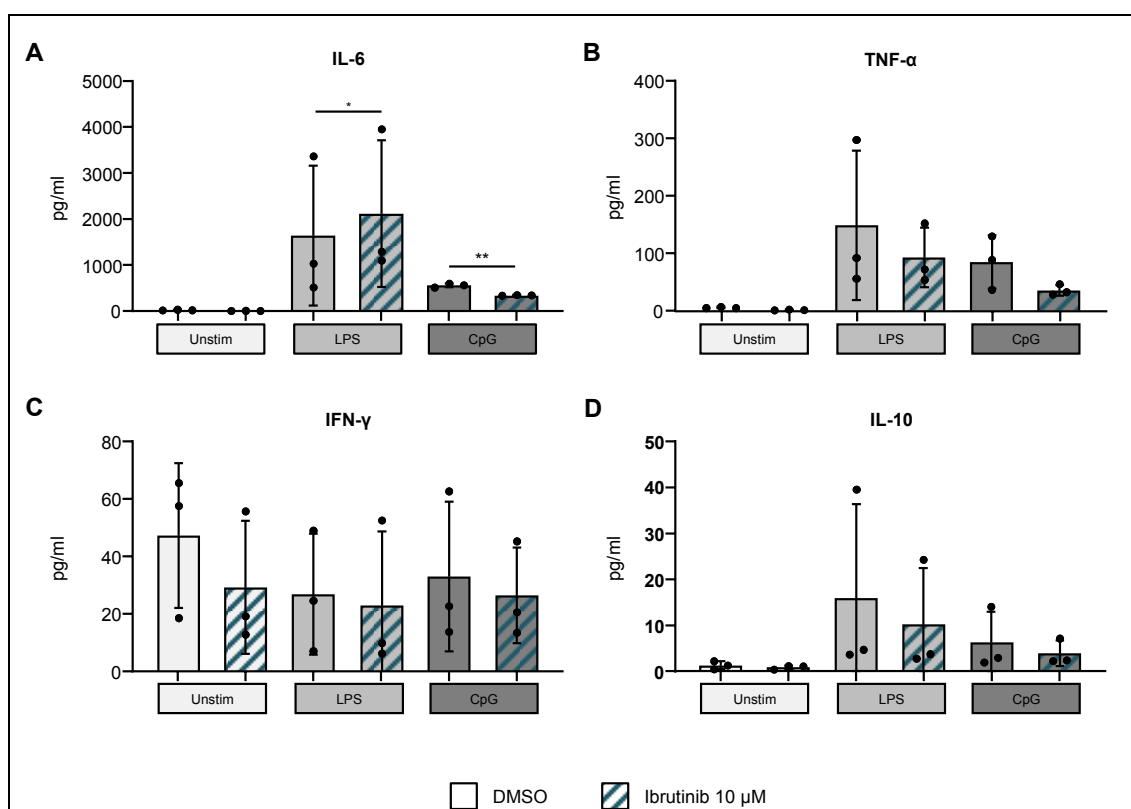
Figure 7: Analysis of cytokine production under LPS- and CpG treatment with ibrutinib treatment in healthy volunteers

Cytokine production of sorted B cells from healthy volunteers was analyzed after 24 hours of culture (*n=3*). **A-D.** Levels of IL-6, TNF-α, IFN-γ and IL-10 are reported for unstimulated, LPS-stimulated and CpG-treated B cells comparing DMSO (control) and ibrutinib treatment (10 µM). Bars represent mean, error bars depict SD. Paired student t-test was used to calculate significance. * = p<0.05, ** = p<0.01.

Consequently, TLR9-stimulation was chosen as a model of autoinflammation as it induced profound changes in the production of cytokines by B cells. Furthermore, stimulation with LPS, which imitates part of the immune reaction in

defense to pathogenic bacteria and, therefore, is often used to model sepsis, showed meaning differences regarding the influence of ibrutinib on B cells.

4.2 Dose-dependent effect of ibrutinib on viability and cytokine production of B cells in healthy volunteers

Thereafter, the effects of ibrutinib on cell viability in relation to the effects on cytokine production were examined in HV over a wide range of concentrations, in order to explain whether the reduced cytokine release was due to limited survival of B cells.

Figure 8: Dose-dependent effect of ibrutinib on viability and cytokine production of B cells in healthy volunteers

Sorted B cells from healthy volunteers were stimulated with CpG and treated with increasing doses of ibrutinib for 24h. **A.** Using counting beads, the absolute survival of B cells in culture was analyzed based on ibrutinib treatment via flow cytometry per 150.000 beads (*n=3*). **B.** A nonlinear regression model of B cell survival relative to the survival in control samples (CpG-stimulated, DMSO-treated). Lines with dots represent three individual trajectories of healthy volunteers. R square = 0.539. **C.** Representative dot plots of one healthy volunteer are shown. Counting beads (red gate) were used as stopping gates, lymphocytes were stained with a viability dye. The percentage of live lymphocytes is indicated for all conditions. **D.** In a Legendplex assay, IL-6 was detected in culture supernatant (*n=3*). Bars represent mean, error bars depict SD. **E.** A nonlinear regression model of IL-6 in culture supernatant relative to control samples (CpG-stimulated, DMSO-treated, *n=3*). Dots represent mean, error bars depict SD.
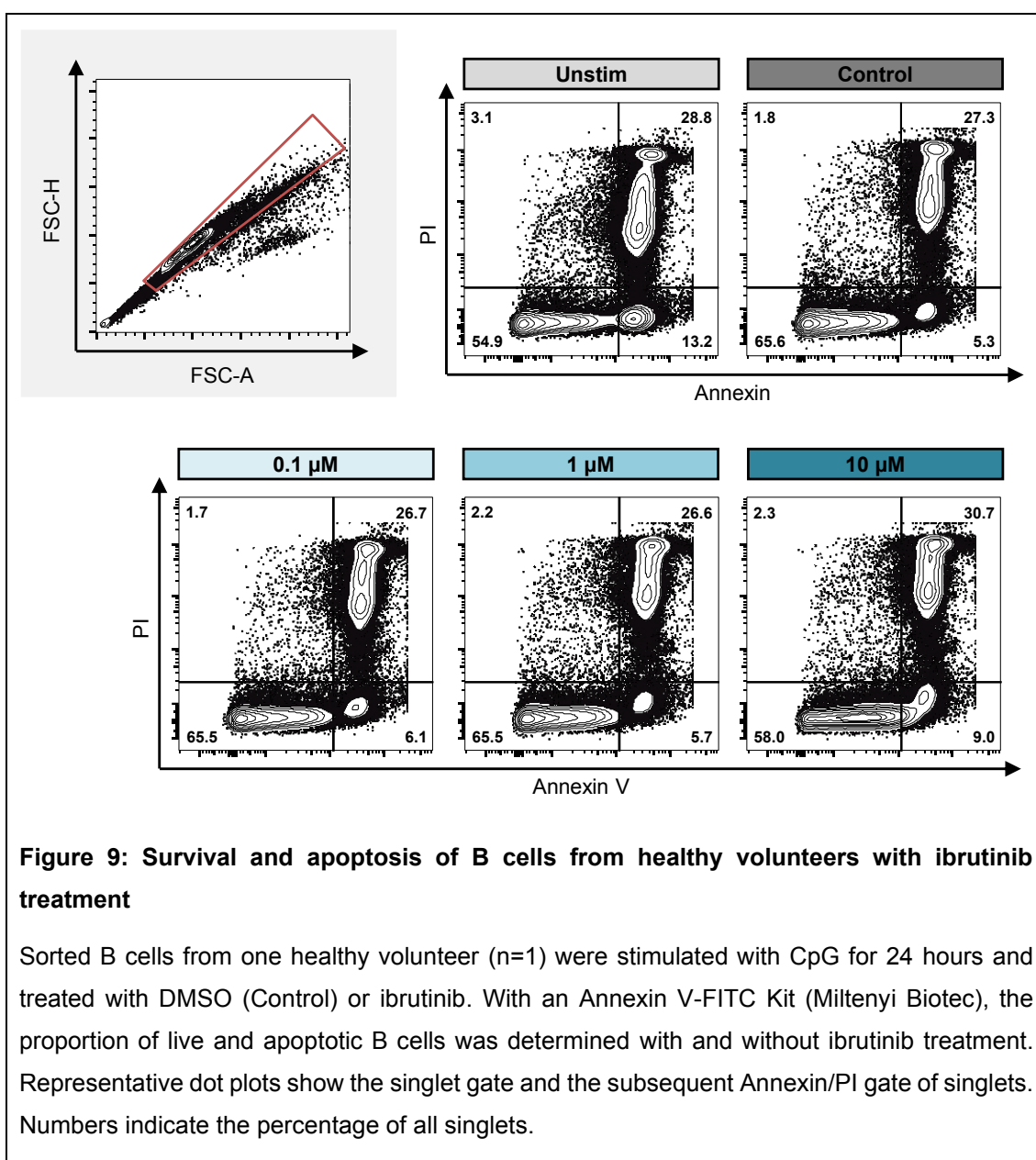
Sorted B cells were cultured with or without CpG-stimulation and with increasing doses of ibrutinib for 24 hours. To evaluate the absolute survival of B cells, counting beads were used as normalization between all samples in order to guarantee a consistent number of events would be recorded for each sample (Figure 8A-C). The fixable viability dye eFluor780 was used to differentiate between living and dead cells. CpG-stimulation increased the number of live B cells by 1.27-fold compared to unstimulated samples. In a dose-dependent manner, higher doses of ibrutinib led to a stronger decrease in detected cell count. At the 10 µM concentration of ibrutinib, the B cell count was finally reduced below the average cell count of unstimulated samples.

Titration of ibrutinib in a Legendplex assay in healthy volunteers showed that the beneficial reduction of IL-6 is already achieved with 0.01 µM of ibrutinib (332.8 ±

20.3 pg/ml compared to 581.5 ± 24.8 pg/ml in DMSO-control samples). Any further dose increase of ibrutinib was not more effective in reducing IL-6.

The dose-dependent effects of ibrutinib both on B cell survival (Figure 8A and C) and the production of IL-6 (Figure 8D) were then modelled with a nonlinear regression model. While the survival curve (R^2 = 0.539) was stable at 0.01 µM and 0.1 µM before sloping down to a relative survival of 0.78 at 10 µM, the fitting curve for IL-6 production (R^2 = 0.784) was almost linear between 0.01 µM and 10 µM ibrutinib at a relative IL-6 production of 0.61, compared to CpG-stimulated, DMSO-treated control samples.

Figure 9: Survival and apoptosis of B cells from healthy volunteers with ibrutinib treatment

Sorted B cells from one healthy volunteer (n=1) were stimulated with CpG for 24 hours and treated with DMSO (Control) or ibrutinib. With an Annexin V-FITC Kit (Miltenyi Biotec), the proportion of live and apoptotic B cells was determined with and without ibrutinib treatment. Representative dot plots show the singlet gate and the subsequent Annexin/PI gate of singlets. Numbers indicate the percentage of all singlets.

While a fixable viability dye can stain necrotic cells, it fails to capture early apoptotic cells undergoing cell death in response to ibrutinib treatment at the timepoint of fixation. Relocation of the phospholipid phosphatidylserine to the outer leaflet of the cell membrane is an early sign of cell death and apoptosis. Annexin V can bind to externalized phosphatidylserine and it can be used as an indicator of ongoing apoptosis. Staining with an Annexin V/Pi Kit was therefore used to differentiate between live (PI⁻Annexin V⁻), early apoptotic (PI⁻Annexin V⁺), late apoptotic (PI⁺Annexin V⁺) and necrotic (PI⁺Annexin V⁻) cells.

CpG-stimulation increased the survival of B cells from 54.8% to 65.8% and reduced the number of apoptotic B cells (Annexin V⁺ PI⁻) by more than half (Figure 9). Low doses of ibrutinib (0.1 µM, 1µM) did not limit B cell survival and only minimally increased the percentage of apoptotic B cells. 10 µM of ibrutinib increased the proportion of B cells undergoing apoptosis, but B cell apoptosis was still lower compared to unstimulated samples.

These experiments showed a dose-dependent effect of ibrutinib on the survival of B cells, while in contrast, the production of IL-6 was reduced to a similar extent with all applied doses of ibrutinib. It's plausible that the inhibition of IL-6 would show a dose-dependency at even lower concentrations close to the determined IC_{50} for BTK inhibition. After this in vitro platform was established and fundamentally important questions concerning cell viability and dose dependency were answered using B cells of healthy volunteers, B cells of patients suffering from SSc were now submitted to the respective functional tests.

4.3 Patient characteristics

Overall, PBMCs from 24 patients were used for in vitro testing (Table 8). Patient and disease characteristics were never consulted as selection criteria for experiments except for the anti-Scl-70 status for the respective experiments.

In our study cohort, 14 patients suffered from lcSSc and 10 patients were diagnosed with dcSSc. Both disease duration (median 8 years, range 1.2 – 24) and mRSS (mean 9.05, range 0 – 44) were highly variably in this patient cohort. Importantly, most patients (75%) did not receive any immunosuppressive therapy at the time of blood draw.

	SSc (n = 24)
DEMOGRAPHICS	
Age - Median - Range	54.0 30-81
Sex - Female - Male	15 (62.5%) 9 (37.5%)
DISEASE CHARACTERISTICS	
SSc subtype - Limited cutaneous SSc - Diffuse cutaneous SSc	14 (58.3%) 10 (41.7%)
Disease duration (years) - Median - Range	8 1.2 – 24
Modified Rodnan Skin Score - Mean - Range	9.05 0 – 44
Pretreatment - Cyclophosphamide - Mycophenolatemofetil - Stem cell transplant	4 (17%) 2 (8%) 2 (8%)
Autoantibodies - Antinuclear antibodies (ANA) - Anti-Scl-70 antibodies - Anti-centromer antibodies (ACA)	4 (17%) 2 (8%) 1 (4%)
Immunosuppressive therapy at time of blood draw - None - Prednisolone - Mycophenolatemofetil - Methotrexate	18 (75%) 2 (8%) 2 (8%) 3 (12%)

Table 8: Patient characteristics of all analysed SSc samples.

This data has in parts been published in Einhaus et al., Arthritis Res. Ther. (2020).

4.4 Dose-dependent effects of ibrutinib on cytokine production by B cells in SSc

To evaluate possible beneficial properties of ibrutinib in the treatment of SSc, the effects on cytokine production of B cells were tested in an in vitro model of autoimmunity. As hypomethylated fragments of DNA can represent a stimulus for autoimmune inflammation in SSc and other rheumatological diseases, the TLR9-agonist CpG was used to induce an innate immune response in B cells. A multiplex assay was chosen to simultaneously analyze the levels of profibrotic IL-6 and TNF-α as well as the amount of immunoregulatory IL-10 and IFN-γ in culture supernatant of purified B cells from patients with SSc after 24 hours. Upon stimulation with CpG, B cells produced 575.9 ± 254.4 pg/ml of IL-6, 95.7 ± 29.7 pg/ml of TNF-α, 4.9 ± 4.6 pg/ml of IFN-γ and 5.7 ± 4.4 pg/ml of IL-10 (Figure 10A-D).

Ibrutinib treatment resulted in decreased IL-6 in the culture supernatant to a similar extent for any applied dose: The levels of profibrotic IL-6 in culture supernatant were decreased to 416.2 ± 128.0 pg/ml with 0.1 µM ibrutinib ($p = 0.0083$), to 414.8 ± 150.6 pg/ml with 1 µM ibrutinib ($p = 0.0079$) and to 380.4 ± 167.5 pg/ml with 10 µM ibrutinib ($p = 0.0023$, Figure 10A). At the same time, TNF-α was reduced by ibrutinib in a dose-dependent manner to 73.9 pg/ml (± 33.1 pg/ml, $p = 0.0187$), 60.9 pg/ml (± 35.5 pg/ml, $p = 0.0042$) and 36.9 pg/ml (± 28.3 pg/ml, $p = 0.0015$), respectively: Higher doses of ibrutinib effected a stronger reduction of TNF-α (Figure 10B). While both IL-6 and TNF-α were already distinctly reduced by the lowest dose of 0.1 µM ibrutinib, the effect on the production of IL-10 and IFN-γ was far less pronounced. A decrease in IFN-γ was only achieved with 10 µM of ibrutinib (3.0 ± 0.6 pg/ml), while no noticeable change was observed at lower concentrations of ibrutinib (Figure 10C). On the other hand, IL-10 was noticeably reduced at 1 µM (4.2 ± 2.2 pg/ml) and 10 µM (3.0 ± 1.4 pg/ml, $p = 0.0105$, Figure 10D).

A IL-6

B TNF-α

C IFN-γ
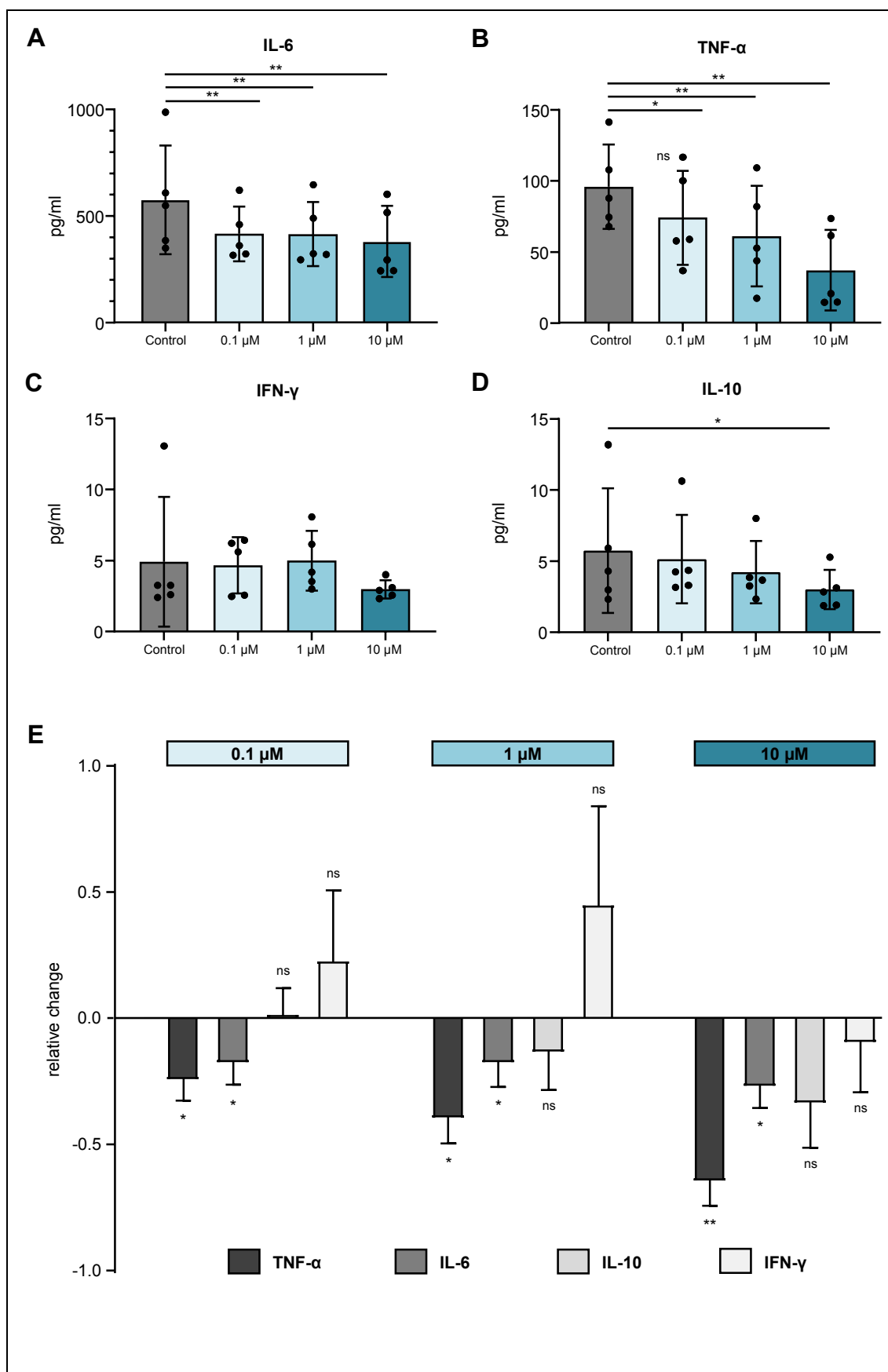
D IL-10

E

Figure 10: Dose-dependent effects of ibrutinib on cytokine production by B cells in SSc

Cytokine production by sorted B cells of patients with SSc was analyzed after 24 hours (*n=5*). **A-D.** Levels of IL-6, TNF-α, IFN-γ and IL-10 are reported for B cells treated with DMSO (control) and ibrutinib (0.1 μM, 1 μM, 10 μM). Bars represent mean, error bars depict SD. ANOVA was used to calculate significance. * = p<0.05, ** = p<0.01. **E.** Relative changes in cytokine levels in the culture supernatant are calculated as fold change (*n=5*). Bars represent mean, error bars depict SEM. One sample t-test was used to calculate significance. * = p<0.05, ** = p<0.01.

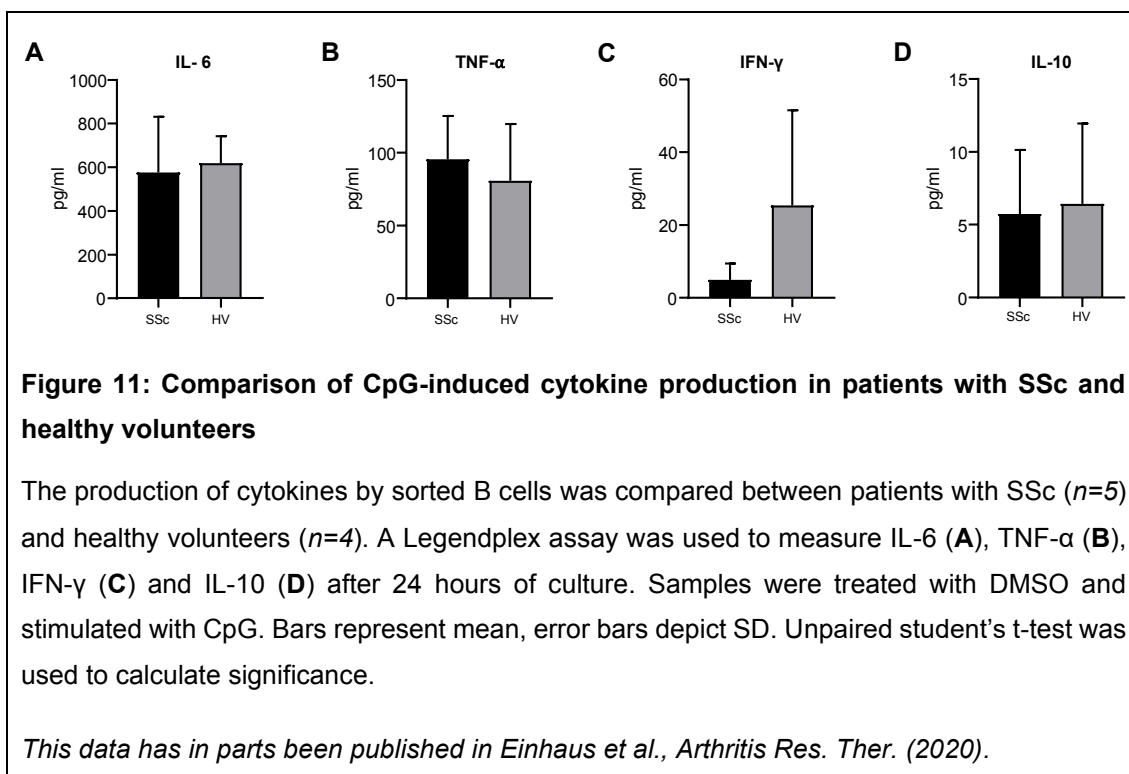*This data has in parts been published in Einhaus et al., Arthritis Res. Ther. (2020).*

The relative changes in cytokine production calculated as fold change comparing to CpG-stimulated DMSO-control samples within each individual patient revealed important differences between the investigated cytokines (Figure 10E). When treated with 0.1 μM ibrutinib, B cells produced significantly less IL-6 and TNF-α (-23.2% and -24.6%, respectively) while the release of IL-10 remained unchanged (+0.0%) and the level of IFN-γ was even increased (+28.7%). In contrast, the highest concentration of ibrutinib (10 μM) lead to an unspecific reduction of all studied cytokines (IL-6: -32.6%, TNF-α: -64.8%, IFN-γ: -9.6%, IL-10: -33.8%).

Thus, ibrutinib reduced the release of the investigated cytokines in an overall dose-dependent manner. In particular low doses of ibrutinib showed differential effects on different cytokines, while high doses of ibrutinib led to reduced cytokine production nonspecifically.

4.5 Comparison of CpG-induced cytokine production in patients with SSc and healthy volunteers

In order to understand the baseline functionality of the cells in the used patient samples, cytokine production by B cells from patients with SSc in response to CpG-stimulation was compared to the release by B cells of healthy volunteers. B cells of four healthy volunteers were cultured in the same way as B cells of

patients with SSc before and cytokines in the supernatant were detected using the same Legendplex assay.

Figure 11: Comparison of CpG-induced cytokine production in patients with SSc and healthy volunteers

The production of cytokines by sorted B cells was compared between patients with SSc (*n=5*) and healthy volunteers (*n=4*). A Legendplex assay was used to measure IL-6 (**A**), TNF-α (**B**), IFN-γ (**C**) and IL-10 (**D**) after 24 hours of culture. Samples were treated with DMSO and stimulated with CpG. Bars represent mean, error bars depict SD. Unpaired student's t-test was used to calculate significance.

This data has in parts been published in Einhaus et al., Arthritis Res. Ther. (2020).
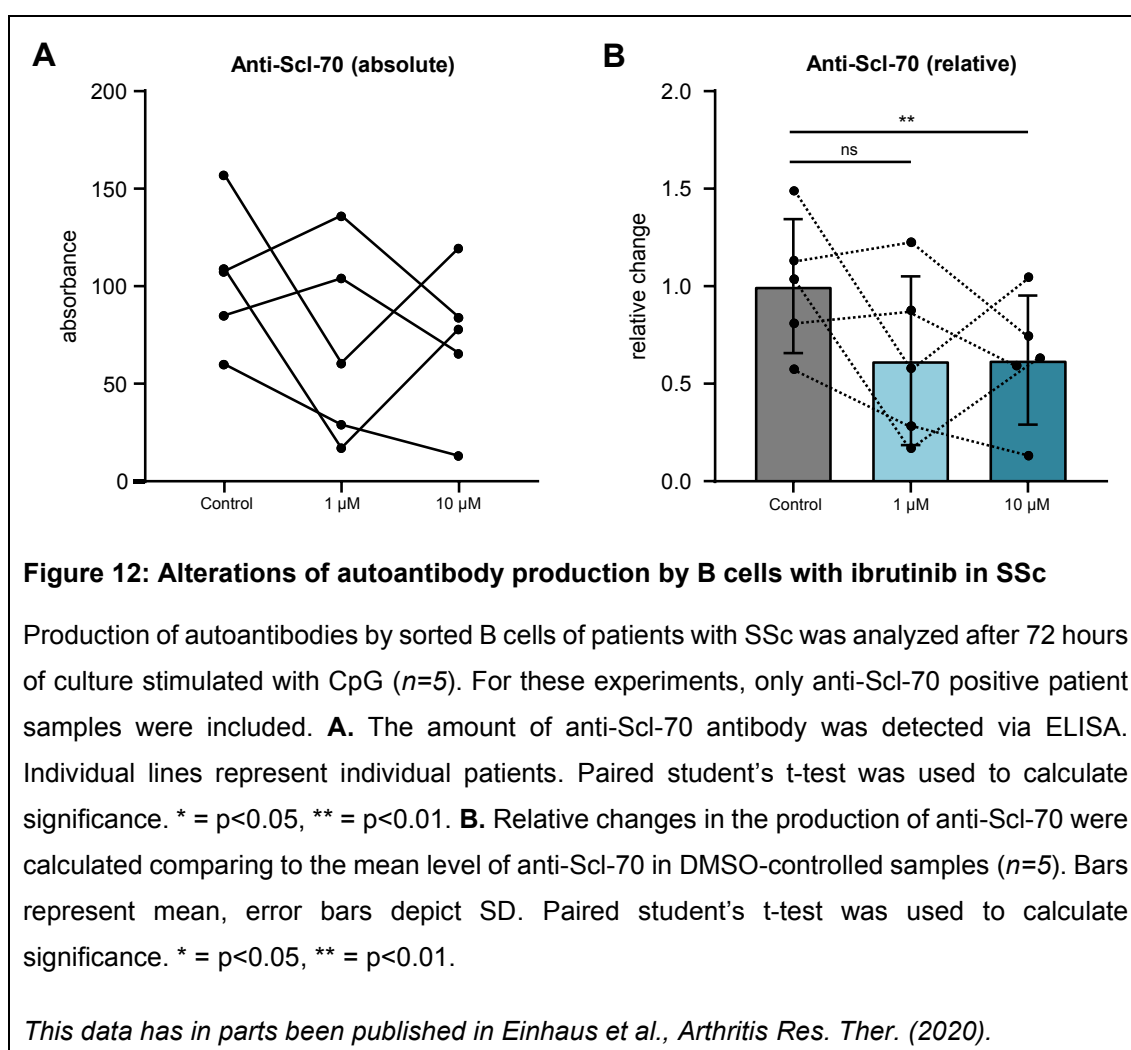
In direct comparison, the average level of IL-6 in culture supernatant of B cells from both patients with SSc and HV corresponded almost perfectly (Figure 11A). Similarly, the amount of TNF-α (Figure 11B) and IL-10 (Figure 11D) were without significant differences between patients with SSc and HV. Interestingly, the levels of IFN-γ (Figure 11C) in B cell cultures from patient samples showed a trend to being decreased compared to HV (4.9 ± 4.6 pg/ml in SSc, 25.4 ± 26.1 pg/ml in HV, p = 0.12).

Overall, cytokine production by B cells was found to be similar between healthy volunteers and patients with SSc.

4.6 Alterations of autoantibody production by B cells with ibrutinib in SSc

In SSc, as in many other autoimmune diseases, autoantibodies can be detected in patient sera via ELISA. Anti-Scl-70 antibodies are most frequently found in patients who suffer from dcSSc and are highly specific for SSc itself, making them a useful diagnostic tool. Instead of a standard curve, our hospital's pathoimmunological laboratory uses anti-Scl-70 positive controls as a reference to evaluate seropositivity for anti-Scl-70 antibodies. Therefore, the difference in absorbance compared to the negative control (B cell medium, background) in absolute and relative numbers was calculated as a measure for relative changes in the production of anti-Scl-70 antibodies.

Figure 12: Alterations of autoantibody production by B cells with ibrutinib in SSc

Production of autoantibodies by sorted B cells of patients with SSc was analyzed after 72 hours of culture stimulated with CpG (*n=5*). For these experiments, only anti-Scl-70 positive patient samples were included. **A.** The amount of anti-Scl-70 antibody was detected via ELISA. Individual lines represent individual patients. Paired student's t-test was used to calculate significance. * = p<0.05, ** = p<0.01. **B.** Relative changes in the production of anti-Scl-70 were calculated comparing to the mean level of anti-Scl-70 in DMSO-controlled samples (*n=5*). Bars represent mean, error bars depict SD. Paired student's t-test was used to calculate significance. * = p<0.05, ** = p<0.01.

This data has in parts been published in Einhaus et al., Arthritis Res. Ther. (2020).

B cells from anti-Scl-70 positive patients were purified, stimulated with CpG and cultured for 72 hours. Via ELISA, anti-Scl-70 was detected in the culture

supernatant. Low dose ibrutinib (1 µM) was not able to unambiguously reduce the level of produced anti-Scl-70. While in two patients, 1 µM ibrutinib dramatically reduced the amount of autoantibody, one individual only showed a slight decrease and two others even an increase in released anti-Scl-70 (Figure 12A). Representation of the fold change in anti-Scl-70 production further elucidates the heterogeneous reaction to ibrutinib treatment (Figure 12B). In contrast, 10 µM ibrutinib consistently reduced the amount of anti-Scl-70 in all samples.

4.7 Subset composition of the B cell compartment and subset-specific reduction of IL-6$^+$ B cells

To further investigate the potentially subset-specific effects of ibrutinib on the cytokine production in B cells, patient PBMCs were incubated for 24 hours and cytokine production was measured via intracellular cytokine staining.
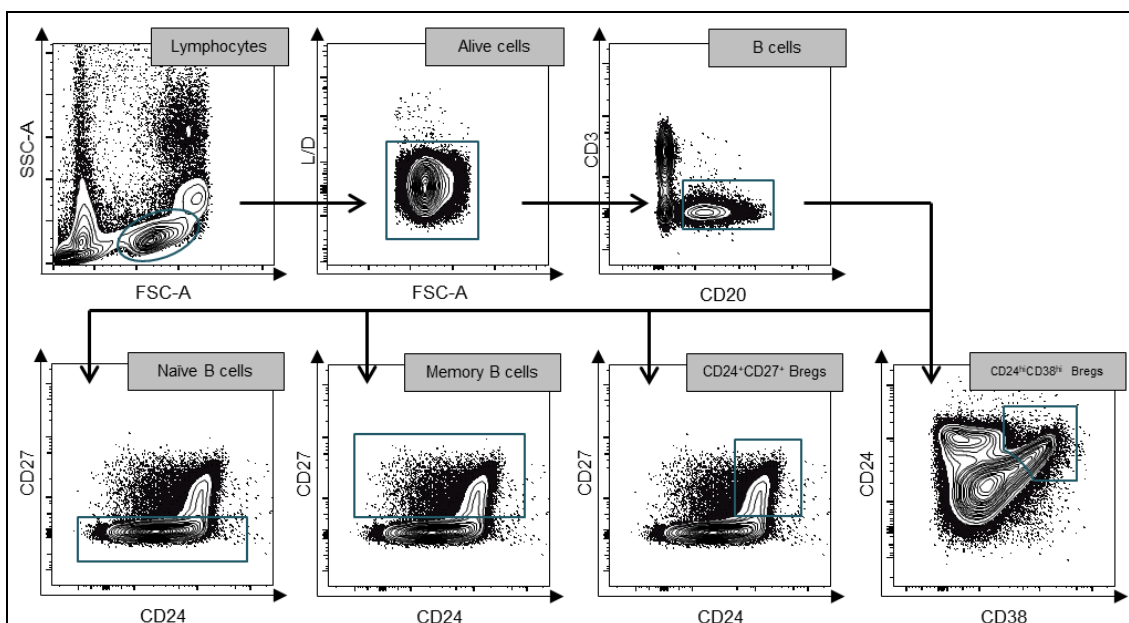
Figure 13: Gating strategy

The gating strategy to identify B cell subpopulations is depicted. In an FSC-A-SSC-A gate, lymphocytes are identified and further specified to live lymphocytes using the L/D staining with Viability Dye. Analyzing CD3 and CD20, B cells are gated as CD3$^-$CD20$^+$ cells. CD27 was used to differentiate between memory (CD27$^+$) and naïve (CD27$^-$) B cells. Regulatory B cells (Bregs) were either gated as CD24$^+$CD27$^+$ or CD24^{hi}CD38^{hi} B cells.

IL-6 was chosen as the profibrotic cytokine of the highest interest and, therefore, the focus of this series of experiments. With ICS, cytokine production can be investigated on a single-cell level, as well as on the level of specific B cell subsets. The gating of B cell subsets was performed as depicted in Figure 13.

Overall, the majority of B cells were classified as naïve B cells (85.6% ± 5.8 %), while memory B cells only accounted for 14.3% (± 5.8%) (Figure 14A). Bregs, which are defined by their ability to release immunoregulatory IL-10, most commonly express the marker combinations CD24^{hi}CD38^{hi} and CD24$^+$CD27$^+$. The gate of CD24^{hi}CD38^{hi} Bregs comprised 8.1% (± 7.5%) of all B cells on average, CD24$^+$CD27$^+$ Bregs accounted for only 3.3% (± 1.5%).

For further analysis, the proportion of IL-6$^+$ cells within the naïve and memory B cell subsets in unstimulated samples and CpG-stimulated samples treated with ibrutinib or DMSO (control) were compared (Figure 14B and C). Without stimulation, only 3.2% (± 1.1%) of naïve B cells were IL-6$^+$. When treated with CpG, IL-6$^+$ naïve B cells were markedly increased to 14.0% (± 9.6%), but consistently reduced after treatment with 1 µM (11.3 ± 7.1%) and 10 µM ibrutinib (10.8 ± 7.9%). The reduction of IL-6$^+$ naïve B cells was significant both with 1 µM (p = 0.027) and 10 µM ibrutinib (p = 0.038). In contrast, more memory B cells (7.3 ± 2.6%) were IL-6$^+$ in unstimulated samples. When stimulated with CpG, a comparable proportion of memory B cells was IL-6$^+$ (13.4 ± 6.2%), but ibrutinib reduced the number significantly only at 10 µM (10.5 ± 4.6%, p = 0.006). Representative dot plots of one patient illustrate the differential effect of ibrutinib at 1 µM on naïve (Figure 14D) and memory (Figure 14E) B cells. Low dose ibrutinib distinctly reduced the proportion of IL-6$^+$ B cells in naïve but not in memory B cells.

Figure 14: Subset composition of the B cell compartment and subset-specific reduction of IL-6+ B cells

PBMCs from patients with SSc were analyzed for subset composition and intracellular IL-6 of the B cell compartment via FACS analysis (*n=10*). **A.** Pie charts represent the mean percentage of naïve (CD27-) and memory (CD27+) B cells as well as CD24hiCD38hi and CD24+CD27+ Bregs of all B cells. **B/C.** The proportions of IL-6+ within the subsets of naïve (**D**) and memory (**E**) B cells were analyzed with and without ibrutinib treatment after 24 hours of stimulation with CpG.

Significance was calculated using a paired student's t-test. Bars represent mean, error bars depict SD. * = p<0.05, ** = p<0.01. **E.** Representative flow cytometry dot plots of one patient. Numbers indicate the percentage of IL-6$^+$ of all naïve B cells. **F.** Representative flow cytometry dot plots of one patient. Numbers indicate the percentage of IL-6$^+$ of all memory B cells all.

This data has in parts been published in Einhaus et al., Arthritis Res. Ther. (2020).

Thus, the phenotypical analysis of ibrutinib-treated PBMCs from patients with SSc revealed that 1 µM of ibrutinib inhibited IL-6 production in naïve but not in memory B cells, whereas 10 µM of ibrutinib lead to a nonspecific inhibition in both subsets.

4.8   Influence of ibrutinib treatment on the B cell subset composition

A number of possible mechanisms could explain the changes in cytokine production in B cells. As the release of the investigated cytokines was differentially influenced by ibrutinib, treatment with ibrutinib could possibly reduce specific cytokines by differentially limiting the survival of certain B cell subsets, e.g. IL-6-producing naïve B cells and IL-10-producing Bregs.
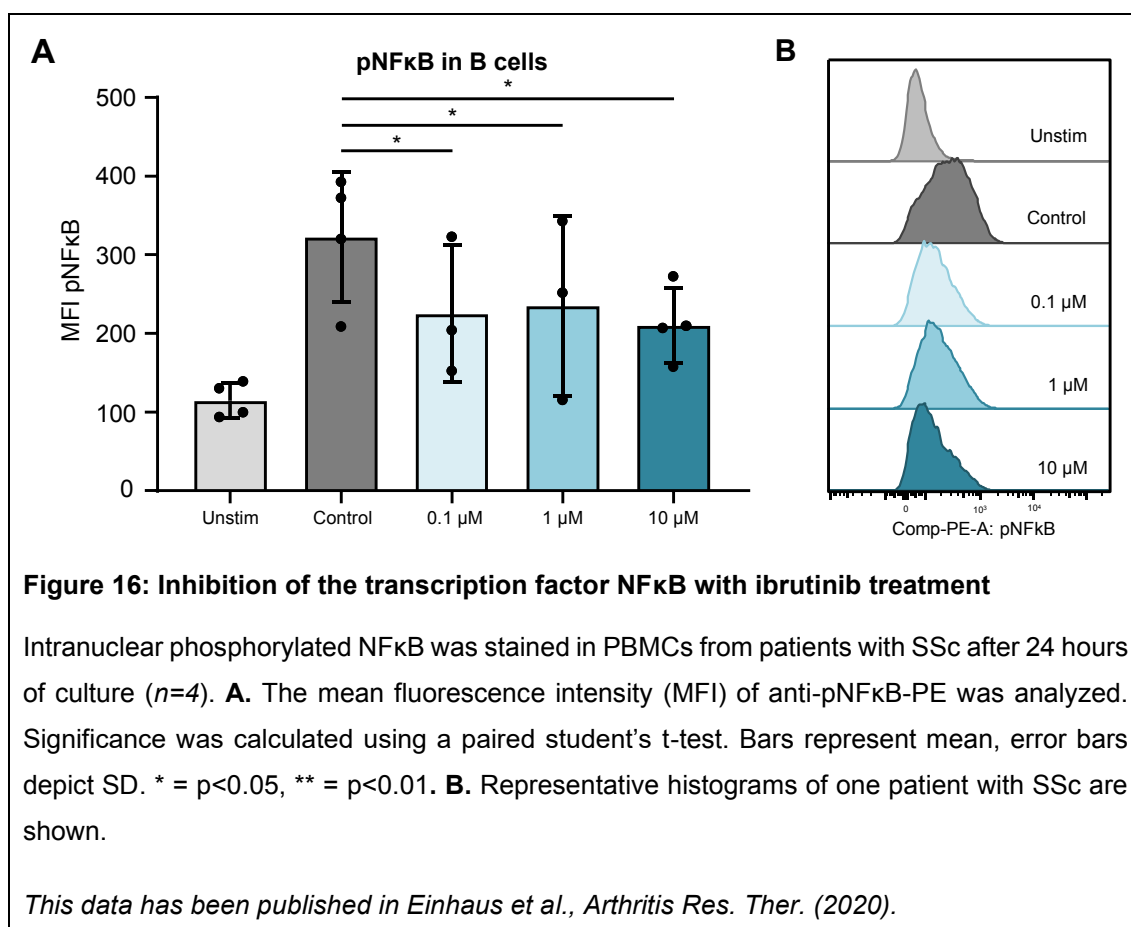
The flow cytometry data of the patient samples analyzed for intracellular cytokine production (paragraph 4.5) was evaluated for dose-dependent changes in the percent composition of B cell subsets. The ratio of B cell subsets in the patients' PBMCs was compared between unstimulated samples and CpG-stimulated samples (DMSO-control, 1 µM ibrutinib, 10 µM ibrutinib).

Figure 15: Influence of ibrutinib treatment on the distribution of B cell subsets

The ratio of different B cell subsets was further analyzed for the influence of ibrutinib treatment on the composition of the B cell compartment (*n=10*). The percentage of naïve B cells (**A**), memory B cells (**B**), CD24^{hi}CD38^{hi} Bregs (**C**) and CD24$^+$CD27$^+$ Bregs (**D**) was analyzed based on stimulation and ibrutinib treatment. Bars represent mean, error bars depict SD.

The proportion of naïve B cells that represented the majority of all B cells in unstimulated samples (85.6 ± 5.8%) showed only minimal differences between CpG-stimulated and ibrutinib-treated samples (Figure 15A). CD27$^+$ memory B cells showed a trend towards reduction with ibrutinib treatment at 10 µM (12.0 ± 6.3%) (Figure 15B). CD24^{hi}CD38^{hi} Bregs accounted for the same percentage of all B cells under all conditions (Figure 15C), while CD24$^+$CD27$^+$ Bregs were slightly reduced when treated with 10 µM ibrutinib (2.6 ± 1.3%) compared to CpG-stimulated controls (3.0 ± 1.5%) (Figure 15D). ANOVA testing confirmed that the differences in the relative subset composition were not significant. Therefore, ibrutinib did not limit the survival of certain B cell subsets differentially.

4.9 Inhibition of the transcription factor NFκB with ibrutinib treatment

NFκB is an important transcription factor in downstream TLR- and BCR-signaling. The target genes of NFκB transcription can boost B cell survival and promote a proinflammatory response to extracellular stimuli. In response to TLR-stimulation, NFκB is of pivotal importance to induce IL-6 production in B cells. Therefore, the level of phosphorylated NFκB (Ser536) was investigated based on CpG-stimulation and ibrutinib treatment in PBMCs from patients with SSc.

Figure 16: Inhibition of the transcription factor NFκB with ibrutinib treatment

Intranuclear phosphorylated NFκB was stained in PBMCs from patients with SSc after 24 hours of culture (*n=4*). **A.** The mean fluorescence intensity (MFI) of anti-pNFκB-PE was analyzed. Significance was calculated using a paired student's t-test. Bars represent mean, error bars depict SD. * = p<0.05, ** = p<0.01. **B.** Representative histograms of one patient with SSc are shown.

This data has been published in Einhaus et al., Arthritis Res. Ther. (2020).

TLR9-stimulation increased the abundance of pNFκB (Ser536) by 2.82-fold at 24 hours of culture, as the MFI was increased from 114.6 ± 22.3 to 322.6 ± 82.6 (Figure 16A and B). Treatment with 0.1 µM ibrutinib was sufficient to significantly reduce the level of pNFκB to 225.7 ± 87.38 (MFI). Higher concentrations of ibrutinib achieved the same decrease in MFI but were not able to reduce the abundance of pNFκB any further.

In summary, this flow cytometry analysis of patient PBMCs showed that ibrutinib reduced the phosphorylation of NFκB in B cells at every concentration from 0.1 µM to 10 µM.

5 Discussion

The BTK gene was identified in 1993 – years after Ogden Bruton had described a case report of a patient with symptoms of a certain immunodeficiency. This condition is known today as agammaglobulinemia, and in the most common subtype (X-linked agammaglobulinemia) it is caused by a complete BTK deficiency, which halts B cell differentiation at the stage of pro-B cells.[80] Soon, the physiological role of the BTK in BCR signaling was characterized, raising an increasing interest in potential inhibitors of BTK function.[81,82] BTK deficiency was found to reduce B cell responsiveness to various B cell activators, such as LPS, CD40, BAFF or IgM, on the level of humoral response and proliferation, making it a target in both autoimmunity and B cell malignancy.[83] In a fast-track approval as a breakthrough therapy, the compound PCI-32765, later named ibrutinib, quickly made its way to clinical application in MCL, CLL, Morbus Waldenstrom and cGvHD. In CLL, ibrutinib is even approved as first-line therapy after it proved superior to the standard first-line therapeutic chlorambucil in a phase III trial.[84]

In single agent regimen, ibrutinib showed proficient tolerability and a low side-effect profile.[85] In previous trials, more than 70% of patients showed transient lymphocytosis which is, however, considered a sign of clinical response.[51,65] Observed adverse reactions (AR) to ibrutinib were mostly grade I or II and typically presented with gastrointestinal, constitutional, respiratory or musculoskeletal symptoms, while severe AR (e.g. neutropenia or thrombocytopenia) occurred only in rare cases.[65] An increased risk for developing atrial fibrillation is observed in 6 - 16% of patients treated with ibrutinib and needs to be addressed appropriately.[86] Currently, ibrutinib treatment is still very expensive with costs of approximately 84,385€ per year as a first-line single therapeutic.[87]

When the first members of this newly discovered class of BTK inhibitor compounds were presented to the public in 2007, the investigators at Celera Genomics did not choose a B cell malignancy but rather the autoimmune disease

RA as their intended clinical application of this drug.[49] However, the transition of ibrutinib in the field of autoimmune diseases remains incomplete. In 2016, phase II clinical trials started testing the BTK inhibitor evobrutinib (M2951) as a treatment for RA (NCT02784106), SLE (NCT02975336) and multiple sclerosis (NCT02975349). Our experiments add to the knowledge of how ibrutinib could be of beneficial impact specifically in SSc.

In this investigation, the effects of ibrutinib on the production of cytokines and the SSc-specific autoantibody anti-Scl-70 by B cells upon stimulation were examined. In general, stimulation of B cells is achieved by binding a specific antigen to the BCR. For autoimmunity, the importance of BCR-TLR9-cooperation has been described, and TLR9 function proved to be indispensable for the detection of self-DNA-fragments.[88,89] Thus, the TLR9 agonist CpG was used to model B cell activation in an autoinflammatory context. Naturally, this in vitro model has certain limitations, as it is insufficient to capture the humoral and cellular complexity of autoimmunity, and it ignores the interplay of immune cells with non-immune cell populations, such as fibroblasts or endothelial cells. Furthermore, it neglects the possibility of B cell stimulation through various simultaneous stimuli or through direct cell-cell interaction. Finally, the in vitro culture was limited to 24 or 72 hours, respectively, examining only a very short period of time during which ibrutinib could effect changes. Despite these limitations, this investigation provides convincing evidence of ibrutinib's great potential to attenuate the pathology of SSc.

In B cells, CpG stimulation induced the production of IL-6 and TNF-α and, to a lesser extent, IFN-γ and IL-10. Hereby, the induced cytokine profile was almost identical for B cells from healthy volunteers and patients with SSc. This assay only examines the potential of B cells to release cytokines upon stimulation, which is not necessarily a predictor for differences in the serum cytokine levels. In the serum of patients with SSc, IL-6 and TNF-α are known to be markedly increased, while IFN-γ was reduced and the level of IL-10 was found to be similar to healthy volunteers.[90] While B cells in our experiments indeed showed a reduced IFN-γ

production upon stimulation, IL-6 and TNF-α in culture supernatant were not increased compared to healthy volunteers. This finding could also be due to differences in sample quality, which would have introduced bias as the patient and healthy volunteer samples were not matched for storage time.

With ibrutinib treatment, B cells produced significantly less IL-6 and TNF-α. Importantly, this effect was achieved most selectively for the profibrotic cytokines at 0.1 µM, a dose that can be reached in patients: 560 mg of orally administered ibrutinib achieves a peak plasma concentration of approximately 130 ng/ml 2h after administration.[50] Thus, with a molecular weight of 440.4971 g/mol, peak ibrutinib concentrations were 0.3 µM, which exceeds by far the IC_{50} of phosphorylation of the BTK's main target PLC-γ (IC_{50} = 29 nM).[66] It was also taken into account that in vivo, 97.7% of ibrutinib is bound to plasma proteins.[91] Human serum was used in all in vitro assays to mirror the availability of ibrutinib in patients as closely as possible.

When assessing the achievements of ibrutinib in the treatment of SSc, it must be critically acknowledged that both rituximab and tocilizumab have failed in previous phase IIb/III trials to substantially improve SSc treatment.[47,92] Nevertheless, B cell-derived IL-6 has proven to be of elementary importance in the formation of germinal centers as well as the accompanied loss of self-tolerance and the generation of autoantibodies.[93] Even though whole B cell-depletion with rituximab or IL-6 antagonism alone, as achieved via tocilizumab, might not be sufficient to improve the outcome of patients with SSc, by changing the most central signaling pathway of B cells with ibrutinib, it seems possible to induce fundamental changes in B cell proliferation, activation and differentiation. In SSc, B cells are assumed to be key players in pathogenesis and disease perpetuation.[1,94] The presence of autoantibodies and general hypergamma-globulinemia is a sign of the pivotal involvement of B cells and can be ascribed to the overexpression of CD19 in SSc leading to amplified BCR-signaling activity. CD19 deficiency on the other hand is linked to reduced IL-6 production by B cells and attenuated skin fibrosis.[30] Therefore, BTK inhibitors could represent the exact

kind of inhibition needed for successful treatment in SSc. A decrease of BTK activity could compensate for the hypersensitivity of BCR-signaling mediated through CD19-overexpression in SSc, and it could be the key to restoring B cell physiology. Our results show that besides reducing proinflammatory IL-6 and TNF-α, ibrutinib also leads to an increase in IFN-γ. This could help to counteract the known deficit of IFN-γ in the serum of patients with SSc. Functionally, IFN-γ is known to have antifibrotic effects by inhibiting collagen synthesis by fibroblasts and inducing collagenase synthesis.[44,95] Contradicting data reporting increased levels of IFN-γ in patients with SSc[38] could therefore represent a reactionary increase of IFN-γ in order to control fibrosis. In summary, ibrutinib could mediate control of fibrosis through both downregulation of profibrotic cytokines and upregulation of antifibrotic mediators.

The production of anti-Scl-70 showed a trend towards lower levels with ibrutinib treatment. This trend, however, was only deducted from measurements of five patient samples and showed great heterogeneity, especially for lower doses of ibrutinib (1 μM). Additional uncertainty was added to this assay because the human plasma used for the cell culture medium proved to contain anti-Scl-70 antibodies, and this background detection had to be subtracted from the absolute values before interpretation. Finally, autoantibodies are produced by very few, single plasma cells that are specific for one type of autoantibody. It is unclear whether an in vitro assay can reliably detect the quantities of autoantibodies produced by these cells. However, considering the mechanism of ibrutinib's inhibition of B cells it still seems likely that the production of autoantibodies would experience a substantial decrease. Usually, autoantibodies are measured in patient sera. Therefore, the effects of ibrutinib on autoantibody production should be revisited when actual patients with SSc received treatment, and potential correlations with clinical parameters can be investigated.

A subset-specific limitation of B cell survival with ibrutinib could have important, potentially beneficial consequences in the treatment of SSc. At baseline without ibrutinib treatment, our results showed that memory B cells were reduced in

numbers, and B cells were largely composed of naïve B cells. This is consistent with previous investigations of B cell composition in SSc.[96] Furthermore, a higher proportion of naïve B cells was IL-6$^+$ than any other investigated B cell subset. This imbalance might be due to the changed cytokine profile in SSc (e.g. increased levels of BAFF which boost the development of premature B cells to naïve mature B cells).[97,98] However, our analysis of the B cell subset composition showed no significant changes with ibrutinib treatment. The influence of ibrutinib probably manifests in early stages of B cell differentiation, persistently shaping B cell proliferation in the bone marrow. Therefore, it is unlikely that these developments can be reliably captured in in vitro experiments after 24h. In a clinical trial, changes in the B cell compartment could be analyzed in patients undergoing ibrutinib treatment in vivo over a longer period of time. Previous investigations in patients with CLL treated with ibrutinib showed that non-malignant B cell numbers were reduced under preservation of the diverse pool of IgH in antigen-primed B cells.[99]

Importantly, ibrutinib was shown to have at most marginal effects on B cell survival in healthy volunteers. Even the highest dose of ibrutinib (10 µM) only decreased the survival to about the same level as in unstimulated controls. This decrease can most likely be ascribed to an ibrutinib-mediated reduced production of factors that promote B cell survival in an autocrine loop. Upon stimulation, B cells release factors (e.g. IL-4, IL-6 and TNF-α) that are known to boost B cell development and survival.[100] Even though complete BTK deficiency is known to increase apoptosis in BCR-stimulated peripheral blood B cells[101], this mechanism seems less relevant regarding SSc ibrutinib treatment given the present data. Particularly in low dose application, in which only minimal effects on B cell viability were detected, ibrutinib-induced apoptosis should not be perceived as a threat to B cell physiology.

The effects of ibrutinib are based on its influence on BCR signaling, where NFκB, NFAT, and ERK are known to be central transcription factors.[62,102,103] In our investigation, we focused on NFκB, as it is a central transcription factor in both

BCR and TLR signaling. NFκB regulates the production of cytokines (IL-1, IL-2, IL-6, IL-8, TNF-α) and anti-apoptotic factors (Fas, BCL-2), profoundly influencing survival, proliferation and inflammatory responses of human immune cells.[104] The activity of NFκB can be modulated via phosphorylation at a number of phosphorylation sites resulting in increased or decreased transcription dependent on phosphorylation site, inflammatory context and cellular location of phosphorylation.[105] Phosphorylation of NFκB at Ser536 within the transactivation domain can enhance its transcriptional activity[106], and in cancer cell lines, a reduction of Ser536 phosphorylation has been linked to lower proliferation rates[107]. However, there is also evidence that pNFκB[Ser536] could be important in limiting NFκB transcription in macrophages.[108] The exact role of pNFκB[Ser536] in B cells cannot be assessed with full certainty. Our results show that ibrutinib treatment significantly reduced the abundance of phosphorylated NFκB. As NFκB is phosphorylated by IKKs that are activated downstream of BTK-dependent BCR- and TLR-signaling[105], decreased levels of pNFκB represent a direct indicator of the downstream effects of BTK inhibition. In further experiments, changes in transcription of individual NFκB target genes such as *IL6* (IL-6), *CXCL8* (IL-8) and *TNFA* (TNF-α) could be measured by mRNA-levels via qPCR in order to evaluate possible gene-specific effects of BTK inhibition.

To further elucidate the potential of ibrutinib in the treatment of SSc, a series of investigations could be undertaken. First, a more sophisticated in vitro model of cocultured fibroblasts and B cells could aid in understanding the influence of ibrutinib on B cell-mediated fibrosis on a molecular level. Specifically, cell-cell-contact dependent mechanisms, as well as humoral effects of B cells on fibroblast cultures, could be examined in a transwell assay. With these experiments, the relevance of ibrutinib-mediated inhibition of profibrotic cytokines could be quantified by measuring changes in collagen synthesis and fibroblast proliferation. TGF-β, a factor typically released by fibroblasts, T cells, macrophages and other cell types, could be added to the panel of detected cytokines because of its important role in SSc.[96,109] As a measure of fibroblast activation, both qPCR for procollagen-mRNA-level as well as western blot for

collagen could be used. In ibrutinib-treated cocultures, a combination of decreased cytokine levels and reduced parameters of fibroblast activation would underscore the potential of ibrutinib to limit pathognomonic features of SSc.

For SSc, a variety of mouse models (e.g. tight skin TSK1/2[+] mouse model, Bleomycin-induced scleroderma mouse model, GvHD alloreactivity mouse models) have been developed, but all are insufficient to recapitulate the complexity of the disease.[96] As the beneficial effects of ibrutinib treatment have already been demonstrated in murine models for GvHD, and the safety of the drug has been evaluated at length, it might be justifiable to apply our preclinical knowledge directly in SSc patients. At first, ibrutinib could be offered to patients as a second- or third-line therapy, when only very limited therapeutic options remain. In this high-risk patient subset, clinical benefits are also most likely to be seen. The clinical trial could be accompanied by a cell biological study investigating the changes and the development of different B cell subsets as well as cytokine and autoantibody levels over time in patients undergoing ibrutinib treatment. An in vivo study is of highest importance as final conclusions about the dynamic of ibrutinib-mediated changes to B cells are more meaningful drawn from in vivo investigations.

Overall, our in vitro data shows the potential of ibrutinib to counteract an underlying pathogenetic immune imbalance of B cells in SSc. This investigation provides convincing evidence that ibrutinib can noticeably improve the B cell pathology that contributes to the onset and progression of SSc and should encourage clinical translation to benefit patients with SSc.

6 Summary

6.1 Summary (English)

Background: SSc is a connective tissue disease that affects skin, blood vessels and internal organs. Symptoms and severity vary from patient to patient, but SSc is often a life-limiting disease due to cardiopulmonary complications. As the pathogenesis of SSc is poorly understood, and causal treatment cannot be provided, therapeutic options are mostly non-curative and strive to alleviate symptoms. B cells have been identified as an important target and a main driver of SSc pathogenesis. Previous attempts to alter B cell pathology (e.g. through B cell-depletion with rituximab) have not proven superior to existing therapies in improving clinical outcomes. Ibrutinib is a small-molecule inhibitor of Bruton's tyrosine kinase (BTK), an important signaling enzyme in B cell receptor (BCR) signaling as well as in other pathways like toll-like receptor (TLR) signaling. In treatment of B cell malignancies, ibrutinib has become invaluable as a first- and second-line therapeutic. Beneficial effects of ibrutinib in autoimmune disease have been postulated, but the transition to clinical application is incomplete.

Methods: We established an in vitro model of autoimmunity in samples of healthy volunteers using unmethylated DNA fragments (CpG) as TLR9 agonists to stimulate B cells and PBMCs. Subsequently, samples of 24 patients with SSc were submitted to functional testing with and without ibrutinib treatment. Here, a Legenplex assay was used to analyze the production of cytokines (IL-6, IL-10, TNF-α, IFN-γ) and an enzyme-linked immunosorbent assay to determine the release of the autoantibody anti-Scl-70. Flow cytometry was used to investigate the phosphorylation of the transcription factor NFκB and the subset composition of B cells with and without ibrutinib treatment.

Results: In samples of healthy volunteers, ibrutinib treatment achieved important changes in cytokine production of CpG-stimulated B cells. Importantly, survival of B cells was reduced noticeably only with high doses of ibrutinib, while cytokine production was already inhibited with much lower concentrations.

Subsequent experiments with samples of patients with SSc showed that B cells from patients with SSc released similar amounts of cytokines upon stimulation with CpG compared to healthy volunteers. In SSc samples, low doses of ibrutinib were able to significantly reduce profibrotic IL-6 and TNF-α, while increasing IFN-γ production by B cells. The level of immunosuppressive IL-10 was unchanged with low doses of ibrutinib. In contrast, high dose ibrutinib led to a nonspecific decrease in all investigated cytokines. Additionally, we also observed a decrease in the production of anti-Scl-70 antibodies with high concentrations of ibrutinib.

Staining of intracellular IL-6 in PBMCs of patients with SSc revealed subset-specific differences in B cell inhibition by ibrutinib. As such, naïve B cells represented the majority of B cells and were more sensitive to low dose ibrutinib treatment compared to the less abundant memory B cells. Importantly, ibrutinib treatment hereby did not alter the composition of B cell subsets in the investigated samples. Finally, the central transcription factor NFκB in its phosphorylated form was significantly reduced in abundance with ibrutinib treatment.

Discussion: Our investigation convincingly demonstrates the potential of ibrutinib to alter B cell pathology in SSc. Specifically, ibrutinib concentrations that can be achieved as clinically relevant serum concentrations in patients show a beneficial constellation of effects. Profibrotic cytokines were found to be reduced, while the levels of anti-inflammatory, immunoregulatory cytokines were preserved. We found indicators of reduced production of autoantibodies and increased immunological responses to bacterial inflammation. This investigation may provide the rationale to test ibrutinib in patients with SSc when other treatments have failed to achieve clinically satisfying improvement.

6.2 Zusammenfassung (Deutsch)

Einleitung: Die Systemische Sklerose (SSc) ist eine Autoimmunerkrankung aus dem Formenkreis der Kollagenosen, die die Haut, Gefäße und innere Organe betrifft. Das klinische Bild variiert stark zwischen Patienten, in schweren Verläufen jedoch kann die SSc vor allem durch kardiopulmonale Komplikationen zum Tode führen. Die Pathogenese der SSc ist nach wie vor weitestgehend unverstanden, weshalb das therapeutische Vorgehen weniger kausal, sondern hauptsächlich symptombezogen Verbesserungen erzielen soll. Die pathologisch veränderte Population der B-Zellen stellt einen möglichen Ansatzpunkt von neuen Therapien dar. Bisherige Versuche, z.B. mit dem anti-CD20-Antikörper Rituximab, haben bisher nicht den erwünschten Erfolg erzielen können. Ibrutinib ist ein Inhibitor der Bruton-Tyrosinkinase (BTK) innerhalb des B-Zell-Rezeptor-Signalwegs und anderer zellulärer Signalkaskaden wie dem TLR-Signalweg. Bei einigen B-Zell-Lymphomen wurden durch eine Behandlung mit Ibrutinib als Therapie erster oder zweiter Wahl bereits große Erfolge erzielt. Auch bei Autoimmunerkrankungen wie der SSc, bei denen B-Zellen eine wichtige Rolle einnehmen, werden positive Effekte durch Ibrutinib vermutet.

Methoden: Das verwendete in vitro Modell für Autoimmunität, in welchem B-Zellen und PBMCs mit unmethylierten DNA-Fragmenten (CpG) stimuliert werden, wurde primär in Proben von gesunden Probanden etabliert.

Anschließend wurden die Effekte von Ibrutinib in 24 Proben von Patienten mit SSc mit verschiedenen Tests analysiert: In einem Legendplex Assay wurde die Produktion verschiedener Zytokine (IL-6, IL-10, TNF-α, IFN-γ) und mittels ELISA die Freisetzung des Autoantikörpers Anti-Scl-70 untersucht.

Durchflusszytometrie wurde verwendet, um den Phosphorylierungsgrad des Transkriptionsfaktors NFκB sowie die Zusammensetzung der B-Zell-Population aus den verschiedenen B-Zell-Subpopulationen zu bestimmen.

Ergebnisse: In den Experimenten mit Proben von gesunden Probanden konnte gezeigt werden, dass Ibrutinib zu einer deutlichen Reduktion der Zytokinproduktion von B-Zellen nach CpG-Stimulation führt. Dabei war die

Überlebensfähigkeit der B-Zellen nur bei hohen Ibrutinibkonzentrationen geringfügig eingeschränkt, während die Zytokinproduktion bereits bei sehr viel geringeren Konzentrationen deutlich vermindert war.

In Experimenten mit SSc-Patientenproben produzierten stimulierte B-Zellen von Patienten mit SSc vergleichbare Mengen der jeweiligen Zytokine wie zuvor B-Zellen der gesunden Probanden. In niedriger Dosierung konnte Ibrutinib die Produktion von profibrotischem IL-6 und TNF-α in B-Zellen deutlich reduzieren, während die Freisetzung von IFN-γ gesteigert wurde. Die Produktion von immunregulatorischem IL-10 durch B-Zellen blieb dabei unverändert. Höhere Konzentrationen an Ibrutinib führten zu einer unspezifischen Verminderung aller untersuchten Zytokine. Außerdem konnte Ibrutinib in hoher Dosierung auch eine verringerte Produktion des Autoantikörpers Anti-Scl-70 erzielen.

Die Färbung von intrazellulärem IL-6 in PBMCs von Patienten mit SSc zeigte die subpopulationsspezifische Wirkung von Ibrutinib: Naïve B-Zellen waren sensibler gegenüber geringen Konzentrationen an Ibrutinib verglichen mit Gedächtnis-B-Zellen. Dabei veränderte Ibrutinib die zahlenmäßige Zusammensetzung der B-Zell-Subpopulationen nicht. Der Phosphorylierungsgrad des Transkriptions-faktor NFκB war in B-Zellen durch Ibrutinib deutlich reduziert.

Diskussion: Unsere Ergebnisse zeigen, dass Ibrutinib die Funktionalität der im Rahmen der SSc pathologisch veränderten B-Zellpopulation grundlegend verändern könnte. Besonders niedrigere, im Patienten erreichbare Konzentrationen an Ibrutinib erzielten eine Kombination aus verschiedenen positiv zu bewertenden Effekten. Diese Ergebnisse stellen einen ersten Schritt in Richtung der klinischen Anwendung von Ibrutinib in Patienten mit SSc dar.

7 References

1. Brown, M. & O'Reilly, S. The immunopathogenesis of fibrosis in systemic sclerosis. *Clin. Exp. Immunol.* **195**, 310–321 (2018).

2. Distler, O. & Cozzio, A. Systemic sclerosis and localized scleroderma—current concepts and novel targets for therapy. *Semin. Immunopathol.* **38**, 87–95 (2016).

3. Tyndall, A. J. *et al.* Causes and risk factors for death in systemic sclerosis: a study from the EULAR Scleroderma Trials and Research (EUSTAR) database. *Ann. Rheum. Dis.* **69**, 1809–1815 (2010).

4. Rubio-Rivas, M., Royo, C., Simeón, C. P., Corbella, X. & Fonollosa, V. Mortality and survival in systemic sclerosis: Systematic review and meta-analysis. *Semin. Arthritis Rheum.* **44**, 208–219 (2014).

5. Elhai, M. *et al.* Mapping and predicting mortality from systemic sclerosis. *Ann. Rheum. Dis.* **76**, 1897–1905 (2017).

6. van den Hoogen, F. *et al.* 2013 Classification Criteria for Systemic Sclerosis: An American College of Rheumatology/European League Against Rheumatism Collaborative Initiative: ACR/EULAR Classification Criteria for SSc. *Arthritis Rheum.* **65**, 2737–2747 (2013).

7. Bissell, L.-A., Abignano, G., Emery, P., Del Galdo, F. & Buch, M. H. Absence of Scleroderma pattern at nail fold capillaroscopy valuable in the exclusion of Scleroderma in unselected patients with Raynaud's Phenomenon. *BMC Musculoskelet. Disord.* **17**, 342 (2016).

8. Mierau, R. *et al.* Frequency of disease-associated and other nuclear autoantibodies in patients of the German network for systemic scleroderma: correlation with characteristic clinical features. *Arthritis Res. Ther.* **13**, R172 (2011).

9. Nihtyanova, S. I. & Denton, C. P. Autoantibodies as predictive tools in systemic sclerosis. *Nat. Rev. Rheumatol.* **6**, 112–116 (2010).

10. Walker, U. A. *et al.* Clinical risk assessment of organ manifestations in systemic sclerosis: a report from the EULAR Scleroderma Trials And Research group database. *Ann. Rheum. Dis.* **66**, 754–763 (2007).

11. Denton, C. P. & Khanna, D. Systemic sclerosis. *The Lancet* **390**, 1685–1699 (2017).

12. Khanna, D. *et al.* Standardization of the Modified Rodnan Skin Score for Use in Clinical Trials of Systemic Sclerosis. *J. Scleroderma Relat. Disord.* **2**, 11–18 (2017).

13. Ramos, P. S., Silver, R. M. & Feghali-Bostwick, C. A. Genetics of systemic sclerosis: recent advances. *Curr. Opin. Rheumatol.* **27**, 521–529 (2015).

14. Feghali-Bostwick, C., Medsger, T. A. & Wright, T. M. Analysis of systemic sclerosis in twins reveals low concordance for disease and high concordance for the presence of antinuclear antibodies. *Arthritis Rheum.* **48**, 1956–1963 (2003).

15. Gorlova, O. *et al.* Identification of Novel Genetic Markers Associated with Clinical Phenotypes of Systemic Sclerosis through a Genome-Wide Association Strategy. *PLoS Genet.* **7**, e1002178 (2011).

16. Kowal-Bielecka, O. *et al.* Update of EULAR recommendations for the treatment of systemic sclerosis. *Ann. Rheum. Dis.* **76**, 1327–1339 (2017).

17. Woodworth, T. G., Suliman, Y. A., Li, W., Furst, D. E. & Clements, P. Scleroderma renal crisis and renal involvement in systemic sclerosis. *Nat. Rev. Nephrol.* **12**, 678–691 (2016).

18. van Laar, J. M. *et al.* Autologous Hematopoietic Stem Cell Transplantation vs Intravenous Pulse Cyclophosphamide in Diffuse Cutaneous Systemic Sclerosis: A Randomized Clinical Trial. *JAMA* **311**, 2490 (2014).

19. Abraham, D. J., Krieg, T., Distler, J. & Distler, O. Overview of pathogenesis of systemic sclerosis. *Rheumatology* **48**, iii3–iii7 (2006).

20. Pleiman, C. M., D'Ambrosio, D. & Cambier, J. C. The B-cell antigen receptor complex: structure and signal transduction. *Immunol. Today* **15**, 393–399 (1994).

21. Melchers, F. The pre-B-cell receptor: selector of fitting immunoglobulin heavy chains for the B-cell repertoire. *Nat. Rev. Immunol.* **5**, 578–584 (2005).

22. LeBien, T. W. & Tedder, T. F. B lymphocytes: how they develop and function. *Blood* **112**, 1570–1580 (2008).

23. Oleinika, K. *et al.* CD1d-dependent immune suppression mediated by regulatory B cells through modulations of iNKT cells. *Nat. Commun.* **9**, 684 (2018).

24. Claes, N., Fraussen, J., Stinissen, P., Hupperts, R. & Somers, V. B Cells Are Multifunctional Players in Multiple Sclerosis Pathogenesis: Insights from Therapeutic Interventions. *Front. Immunol.* **6**, 642 (2015).

25. Maecker, H. T., McCoy, J. P. & Nussenblatt, R. Standardizing immunophenotyping for the Human Immunology Project. *Nat. Rev. Immunol.* **12**, 191–200 (2012).

26. Sato, S., Fujimoto, M., Hasegawa, M. & Takehara, K. Altered blood B lymphocyte homeostasis in systemic sclerosis: Expanded naive B cells and diminished but activated memory B cells. *Arthritis Rheum.* **50**, 1918–1927 (2004).

27. Sato, S., Hasegawa, M., Fujimoto, M., Tedder, T. F. & Takehara, K. Quantitative Genetic Variation in CD19 Expression Correlates with Autoimmunity. *J. Immunol.* **165**, 6635–6643 (2000).

28. Inaoki, M., Sato, S., Weintraub, B. C., Goodnow, C. C. & Tedder, T. F. CD19-Regulated Signaling Thresholds Control Peripheral Tolerance and Autoantibody Production in B Lymphocytes. *J. Exp. Med.* **186**, 1923–1931 (1997).

29. Asano, N. *et al.* B Lymphocyte Signaling Established by the CD19/CD22 Loop Regulates Autoimmunity in the Tight-Skin Mouse. *Am. J. Pathol.* **165**, 641–650 (2004).

30. Saito, E. *et al.* CD19-dependent B lymphocyte signaling thresholds influence skin fibrosis and autoimmunity in the tight-skin mouse. *J. Clin. Invest.* **109**, 1453–1462 (2002).

31. Baroni, S. S., Luchetti, M., Fraticelli, P., Kazlauskas, A. & Gabrielli, A. Stimulatory Autoantibodies to the PDGF Receptor in Systemic Sclerosis. *N. Engl. J. Med.* **354**, 2667-2676 (2006).

32. Hénault, J., Tremblay, M., Clément, I., Raymond, Y. & Senécal, J.-L. Direct binding of anti-DNA topoisomerase I autoantibodies to the cell surface of fibroblasts in patients with systemic sclerosis: Antifibroblast Autoantibodies in SSc. *Arthritis Rheum.* **50**, 3265–3274 (2004).

33. Matsushita, T. Regulatory and effector B cells: Friends or foes? *J. Dermatol. Sci.* **93**, 2–7 (2019).

34. Matsushita, T., Hamaguchi, Y., Hasegawa, M., Takehara, K. & Fujimoto, M. Decreased levels of regulatory B cells in patients with systemic sclerosis: association with autoantibody production and disease activity. *Rheumatology* **55**, 263–267 (2016).

35. Iwata, Y. *et al.* Characterization of a rare IL-10-competent B-cell subset in humans that parallels mouse regulatory B10 cells. *Blood* **117**, 530–541 (2011).

36. Rosser, E. C. & Mauri, C. Regulatory B Cells: Origin, Phenotype, and Function. *Immunity* **42**, 607–612 (2015).

37. Blair, P. A. *et al.* CD19+CD24hiCD38hi B Cells Exhibit Regulatory Capacity in Healthy Individuals but Are Functionally Impaired in Systemic Lupus Erythematosus Patients. *Immunity* **32**, 129–140 (2010).

38. Gourh, P. *et al.* Plasma cytokine profiles in systemic sclerosis: associations with autoantibody subsets and clinical manifestations. *Arthritis Res. Ther.* **11**, R147 (2009).

39. Kawaguchi, Y. Contribution of Interleukin-6 to the Pathogenesis of Systemic Sclerosis. *J. Scleroderma Relat. Disord.* **2**, S6–S12 (2017).

40. O'Reilly, S., Cant, R., Ciechomska, M. & van Laar, J. M. Interleukin-6: a new therapeutic target in systemic sclerosis? *Clin. Transl. Immunol.* **2**, e4 (2013).

41. Khanna, D. *et al.* Safety and efficacy of subcutaneous tocilizumab in adults with systemic sclerosis (faSScinate): a phase 2, randomised, controlled trial. *The Lancet* **387**, 2630–2640 (2016).

42. Denton, C. P. *et al.* An open-label pilot study of infliximab therapy in diffuse cutaneous systemic sclerosis. *Ann. Rheum. Dis.* **68**, 1433–1439 (2009).

43. Rieckmann, P., D'Alessandro, F., Nordan, R. P., Fauci, A. S. & Kehrl, H. IL-6 and tumor necrosis factor-alpha. Autocrine and paracrine cytokines involved in B cell function. *J. Immunol.* **146**, 3462–2468 (1991).

44. Rosenbloom, J., Feldman, G., Freundlich, B. & Jimenez, S. Rosenbloom et al. - 1984 - Transcriptional control of human diploid fibroblast collagen synthesis by IFN-gamma.pdf. *Biochem. Biophys. Res. Commun.* **123**, 365–372 (1984).

45. Chizzolini, C. *et al.* Inhibition of type I collagen production by dermal fibroblasts upon contact with activated T cells: Different sensitivity to inhibition between systemic sclerosis and control fibroblasts. *Arthritis Rheum.* **41**, 2039–2047 (1998).

46. Pattanaik, D., Brown, M., Postlethwaite, B. C. & Postlethwaite, A. E. Pathogenesis of Systemic Sclerosis. *Front. Immunol.* **6**, 272 (2015).

47. Jordan, S. *et al.* Effects and safety of rituximab in systemic sclerosis: an analysis from the European Scleroderma Trial and Research (EUSTAR) group. *Ann. Rheum. Dis.* **74**, 1188–1194 (2015).

48. Matsushita, T. *et al.* BAFF inhibition attenuates fibrosis in scleroderma by modulating the regulatory and effector B cell balance. *Sci. Adv.* **4**, eaas9944 (2018).

49. Pan, Z. *et al.* Discovery of Selective Irreversible Inhibitors for Bruton's Tyrosine Kinase. *ChemMedChem* **2**, 58–61 (2007).

50. Advani, R. H. *et al.* Bruton Tyrosine Kinase Inhibitor Ibrutinib (PCI-32765) Has Significant Activity in Patients With Relapsed/Refractory B-Cell Malignancies. *J. Clin. Oncol.* **31**, 88–94 (2013).

51. Byrd, J. C. *et al.* Targeting BTK with Ibrutinib in Relapsed Chronic Lymphocytic Leukemia. *N. Engl. J. Med.* **369**, 32–42 (2013).

52. Dreyling, M. *et al.* Ibrutinib versus temsirolimus in patients with relapsed or refractory mantle-cell lymphoma: an international, randomised, open-label, phase 3 study. *The Lancet* **387**, 770–778 (2016).

53. Allen, J. L. *et al.* B cells from patients with chronic GVHD are activated and primed for survival via BAFF-mediated pathways. *Blood* **120**, 2529–2536 (2012).

54. Sarantopoulos, S. *et al.* Altered B-cell homeostasis and excess BAFF in human chronic graft-versus-host disease. *Blood* **113**, 3865–3874 (2009).

55. Shimabukuro-Vornhagen, A., Hallek, M. J., Storb, R. F. & von Bergwelt-Baildon, M. S. The role of B cells in the pathogenesis of graft-versus-host disease. *Blood* **114**, 4919–4927 (2009).

56. Dubovsky, J. A. *et al.* Ibrutinib treatment ameliorates murine chronic graft-versus-host disease. *J. Clin. Invest.* **124**, 4867–4876 (2014).

57. Miklos, D. *et al.* Ibrutinib for chronic graft-versus-host disease after failure of prior therapy. *Blood* **130**, 2243–2250 (2017).

58. Nutt, S. L., Hodgkin, P. D., Tarlinton, D. M. & Corcoran, L. M. The generation of antibody-secreting plasma cells. *Nat. Rev. Immunol.* **15**, 160–171 (2015).

59. Marshak-Rothstein, A. Toll-like receptors in systemic autoimmune disease. *Nat. Rev. Immunol.* **6**, 823–835 (2006).

60. Viglianti, G. A. *et al.* Activation of Autoreactive B Cells by CpG dsDNA. *Immunity* **19**, 837–847 (2003).

61. Pone, E. J. *et al.* BCR-signalling synergizes with TLR-signalling for induction of AID and immunoglobulin class-switching through the non-canonical NF-κB pathway. *Nat. Commun.* **3**, 767 (2012).

62. Merolle, M. I., Ahmed, M., Nomie, K. & Wang, M. L. The B cell receptor signaling pathway in mantle cell lymphoma. *Oncotarget* **9**, 25332-25341 (2018).

63. Vetrie, D. *et al.* The gene involved in X-linked agammaglobulinaemia is a member of the src family of protein-tyrosine kinases. **361**, 8 (1993).

64. Mizuno, T. & Rothstein, T. L. B Cell Receptor (BCR) Cross-Talk: CD40 Engagement Creates an Alternate Pathway for BCR Signaling That Activates IκB Kinase/IκBα/NF-κB without the Need for PI3K and Phospholipase Cγ. *J. Immunol.* **174**, 6062–6070 (2005).

65. Wang, Y., Zhang, L., Champlin, R. & Wang, M. Targeting Bruton's tyrosine kinase with ibrutinib in B-cell malignancies. *Clin. Pharmacol. Ther.* **97**, 455–468 (2015).

66. Honigberg, L. A. *et al.* The Bruton tyrosine kinase inhibitor PCI-32765 blocks B-cell activation and is efficacious in models of autoimmune disease and B-cell malignancy. *Proc. Natl. Acad. Sci.* **107**, 13075–13080 (2010).

67. Akira, S., Uematsu, S. & Takeuchi, O. Pathogen Recognition and Innate Immunity. *Cell* **124**, 783–801 (2006).

68. Krieg, A. M. *et al.* CpG motifs in bacterial DNA trigger direct B-cell activation. *Nature* **374**, 546–549 (1995).

69. Fang, F. *et al.* Toll-like Receptor 9 Signaling Is Augmented in Systemic Sclerosis and Elicits Transforming Growth Factor β-Dependent Fibroblast Activation: TLR9 SIGNALING PROMOTES FIBROTIC RESPONSES. *Arthritis Rheumatol.* **68**, 1989–2002 (2016).

70. Laurent, P. *et al.* Innate Immunity in Systemic Sclerosis Fibrosis: Recent Advances. *Front. Immunol.* **9**, 1702 (2018).

71. Altorok, N., Tsou, P.-S., Coit, P., Khanna, D. & Sawalha, A. H. Genome-wide DNA methylation analysis in dermal fibroblasts from patients with diffuse and limited systemic sclerosis reveals common and subset-specific DNA methylation aberrancies. *Ann. Rheum. Dis.* **74**, 1612–1620 (2015).

72. Lei, W. *et al.* Abnormal DNA methylation in CD4+ T cells from patients with systemic lupus erythematosus, systemic sclerosis, and dermatomyositis. *Scand. J. Rheumatol.* **38**, 369–374 (2009).

73. Leadbetter, E. A. *et al.* Chromatin–IgG complexes activate B cells by dual engagement of IgM and Toll-like receptors. *Nature* **416**, 603–607 (2002).

74. Latz, E. *et al.* TLR9 signals after translocating from the ER to CpG DNA in the lysosome. *Nat. Immunol.* **5**, 190–198 (2004).

75. Lin, S.-C., Lo, Y.-C. & Wu, H. Helical assembly in the MyD88–IRAK4–IRAK2 complex in TLR/IL-1R signalling. *Nature* **465**, 885–890 (2010).

76. Kawasaki, T. & Kawai, T. Toll-Like Receptor Signaling Pathways. *Front. Immunol.* **5**, 461 (2014).

77. Doyle, S. L., Jefferies, C. A., Feighery, C. & O'Neill, L. A. J. Signaling by Toll-like Receptors 8 and 9 Requires Bruton's Tyrosine Kinase. *J. Biol. Chem.* **282**, 36953–36960 (2007).

78. Lee, K.-G., Xu, S., Wong, E.-T., Tergaonkar, V. & Lam, K.-P. Bruton's Tyrosine Kinase Separately Regulates NFκB p65RelA Activation and Cytokine Interleukin (IL)-10/IL-12 Production in TLR9-stimulated B Cells. *J. Biol. Chem.* **283**, 11189–11198 (2008).

79. Du, B., Jiang, Q.-L., Cleveland, J., Liu, B.-R. & Zhang, D. Targeting Toll-like receptors against cancer. *J. Cancer Metastasis Treat.* **2**, 463 (2016).

80. Smith, C. I. E. From identification of the BTK kinase to effective management of leukemia. *Oncogene* **36**, 2045–2053 (2017).

81. Rawlings, D. J. *et al.* Activation of BTK by a Phosphorylation Mechanism Initiated by SRC Family Kinases. *Science* **271**, 822–825 (1996).

82. Takata, M. & Kurosaki, T. A Role for Bruton's Tyrosine Kinase in B Cell Antigen Receptor-mediated Activation of Phospholipase C-γ2. *J. Exp. Med.* **184**, 31–40 (1996).

83. Khan, W. N. *et al.* Defective B Cell Development and Function in Bfk-Deficient Mice. **3**, 283-299 (1995).

84. Burger, J. A. *et al.* Ibrutinib as Initial Therapy for Patients with Chronic Lymphocytic Leukemia. *N. Engl. J. Med.* **373**, 2425–2437 (2015).

85. Coutre, S. E. *et al.* Long-term safety of single-agent ibrutinib in patients with chronic lymphocytic leukemia in 3 pivotal studies. *Blood Adv.* **3**, 1799–1807 (2019).

86. Brown, J. R. *et al.* Characterization of atrial fibrillation adverse events reported in ibrutinib randomized controlled registration trials. *Haematologica* **102**, 1796–1805 (2017).

87. G-BA. Gemeinsamer Bundesausschuss: Beschlusstext des Gemeinsamen Bundesausschusses über eine Änderung der Arzneimittel-Richtlinie (AM-RL): Anlage XII - Beschlüsse über die Nutzenbewertung von Arzneimitteln mit neuen Wirkstoffen nach § 35a SGB V – Ibrutinib (neues Anwendungsgebiet). Beschlussdatum: 15.12.2016. https://www.g-ba.de/downloads/39-261-2797/2016-12-15_AM-RL-XII_Ibrutinib_nAWG_D-249_BAnz.pdf (Stand: 20.04.2020)

88. Suthers, A. N. & Sarantopoulos, S. TLR7/TLR9- and B Cell Receptor-Signaling Crosstalk: Promotion of Potentially Dangerous B Cells. *Front. Immunol.* **8**, 775 (2017).

89. Minton, K. BCR and TLR9 cooperation in autoimmunity. *Nat. Rev. Immunol.* **4**, 82–82 (2004).

90. Scala, E. *et al.* Cytokine and chemokine levels in systemic sclerosis: relationship with cutaneous and internal organ involvement. *Clin. Exp. Immunol.* **138**, 540–546 (2004).

91. Scheers, E. *et al.* Absorption, Metabolism, and Excretion of Oral [14]C Radiolabeled Ibrutinib: An Open-Label, Phase I, Single-Dose Study in Healthy Men. *Drug Metab. Dispos.* **43**, 289–297 (2015).

92. Khanna, D. *et al.* Efficacy and Safety of Tocilizumab for the Treatment of Systemic Sclerosis: Results from a Phase 3 Randomized Controlled Trial. [abstract]. Arthritis Rheumatol. 2018; 70 (suppl 10).

93. Arkatkar, T. *et al.* B cell–derived IL-6 initiates spontaneous germinal center formation during systemic autoimmunity. *J. Exp. Med.* **214**, 3207–3217 (2017).

94. Sanges, S. *et al.* Role of B cells in the pathogenesis of systemic sclerosis. *Rev. Médecine Interne* **38**, 113–124 (2017).

95. Baraut, J., Michel, L., Verrecchia, F. & Farge, D. Relationship between cytokine profiles and clinical outcomes in patients with systemic sclerosis. *Autoimmun. Rev.* **10**, 65–73 (2010).

96. Katsumoto, T. R., Whitfield, M. L. & Connolly, M. K. The Pathogenesis of Systemic Sclerosis. *Annu. Rev. Pathol. Mech. Dis.* **6**, 509–537 (2011).

97. Schweighoffer, E. & Tybulewicz, V. L. Signalling for B cell survival. *Curr. Opin. Cell Biol.* **51**, 8–14 (2018).

98. Mackay, F. & Browning, J. L. BAFF: A fundamental survival factor for B cells. *Nat. Rev. Immunol.* **2**, 465–475 (2002).

99. Schliffke, S. *et al.* Dynamic changes of the normal B lymphocyte repertoire in CLL in response to ibrutinib or FCR chemo-immunotherapy. *OncoImmunology* **7**, e1417720 (2018).

100. Herman, S. E. M. *et al.* Bruton tyrosine kinase represents a promising therapeutic target for treatment of chronic lymphocytic leukemia and is effectively targeted by PCI-32765. *Blood* **117**, 6287–6296 (2011).

101. Anderson, J. S., Teutsch, M., Dong, Z. & Wortis, H. H. An essential role Bruton's tyrosine kinase in the regulation of B-cell apoptosis. *Proc Natl Acad Sci USA* **93,** 10966–10971 (1996).

102. Woyach, J. A., Johnson, A. J. & Byrd, J. C. The B-cell receptor signaling pathway as a therapeutic target in CLL. *Blood* **120**, 1175–1184 (2012).

103. Niemann, C. U. & Wiestner, A. B-cell receptor signaling as a driver of lymphoma development and evolution. *Semin. Cancer Biol.* **23**, 410–421 (2013).

104. Liu, T., Zhang, L., Joo, D. & Sun, S.-C. NF-κB signaling in inflammation. *Signal Transduct. Target. Ther.* **2**, e17023 (2017).

105. Christian, F., Smith, E. & Carmody, R. The Regulation of NF-κB Subunits by Phosphorylation. *Cells* **5**, 12 (2016).

106. Chen, L.-F. *et al.* NF- B RelA Phosphorylation Regulates RelA Acetylation. *Mol. Cell. Biol.* **25**, 7966–7975 (2005).

107. Adli, M. & Baldwin, A. S. IKK-i/IKKε Controls Constitutive, Cancer Cell-associated NF-κB Activity via Regulation of Ser-536 p65/RelA Phosphorylation. *J. Biol. Chem.* **281**, 26976–26984 (2006).

108. Lawrence, T., Bebien, M., Liu, G. Y., Nizet, V. & Karin, M. IKKa limits macrophage NF-kB activation and contributes to the resolution of inflammation. **434**, 6 (2005).

109. Varga, J. & Pasche, B. Transforming growth factor β as a therapeutic target in systemic sclerosis. *Nat. Rev. Rheumatol.* **5**, 200–206 (2009).

8   Lists of tables and figures

8.1   Tables

8.2   Figures

9   Declaration of authorship

I, Jakob Einhaus, designed and performed all experiments for the figures 5-15, analyzed the data and wrote the manuscript for publication (Einhaus et al. 2020). I personally designed all figures based on the generated data or based on information from the respective references.

Elisa Asteriti, Hannes Schmid, Silke Duerr-Stoerzer, Hildegard Keppeler and Kathy-Ann Secker helped processing patient samples for PBMCs extraction.

Joerg Henes and Ann-Christin Pecher recruited patients and obtained written consent from each individual patient.

Reinhild Klein, Corinna Schneidawind and Joerg Henes helped interpreting the data and assisted in preparing the manuscript for publication (Einhaus et al. 2020).

Dominik Schneidawind designed and supervised the experiments, read and approved the manuscript and provided overall guidance.

I affirm that I myself have written this manuscript and I affirm that I have not used any other references than the ones indicated.

Tübingen, 20.04.2020

10 Publications

Einhaus, J., Pecher, A., Asteriti, E., Schmid, H., Secker, KA., Duerr-Stoerzer, S., Keppeler, H., Klein, R., Schneidawind, C., Schneidawind, D., **2020**. Inhibition of effector B cells by ibrutinib in systemic sclerosis. *Arthritis Res Ther* 22:66. https://doi.org/10.1186/s13075-020-02153-8

11 Acknowledgment

I would like to express my sincere gratitude to my supervisor PD Dr. Dominik Schneidawind for all the continuous guidance, support, and encouragement throughout this research project.

I would like to thank Hannes Schmid, Kathy-Ann Secker, Hildegard Keppeler, Silke Dürr-Störzer and Gülay Demirel for their support and advice during the experimental work. A special thank you also goes to Dyani Gaudilliere for the helpful feedback during the writing of this thesis.

Most of all, I would like to thank my family: Friedrich, Andrea, Johanna and Antonia. You are simply the best.